HAL open science

Liquid-vapour transition of the long range Yukawa fluid.

Jean-Jacques Weis, Lo Verso Federica, Caillol Jean-Michel, Schoell-Paschinger Elisabeth

To cite this version:

Jean-Jacques Weis, Lo Verso Federica, Caillol Jean-Michel, Schoell-Paschinger Elisabeth. Liquid-vapour transition of the long range Yukawa fluid.. Molecular Physics, 2007, 105 (13-14), pp.1813-1826. 10.1080/00268970701420524 . hal-00513105

HAL Id: hal-00513105

https://hal.science/hal-00513105v1

Submitted on 1 Sep 2010

HAL is a multi-disciplinary open access archive for the deposit and dissemination of scientific research documents, whether they are published or not. The documents may come from teaching and research institutions in France or abroad, or from public or private research centers.

L'archive ouverte pluridisciplinaire **HAL**, est destinée au dépôt et à la diffusion de documents scientifiques de niveau recherche, publiés ou non, émanant des établissements d'enseignement et de recherche français ou étrangers, des laboratoires publics ou privés.

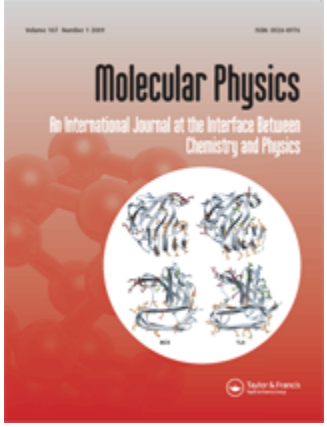

Liquid-vapour transition of the long range Yukawa fluid.

Journal:	*Molecular Physics*
Manuscript ID:	TMPH-2007-0081.R1
Manuscript Type:	Full Paper
Date Submitted by the Author:	24-Apr-2007
Complete List of Authors:	Weis, Jean-Jacques; Laboratoire de Physique Théorique, Université Paris-Sud Federica, Lo Verso; Institut fur Theoretische Physik, Heinrich-Heine-Universitat Jean-Michel, Caillol; Laboratoire de Physique Théorique, Université Paris-Sud Elisabeth, Schoell-Paschinger; CMS and Fakultaet fur Physik, Universitaet Wien
Keywords:	Yukawa potential, Critical Phenomena, Monte Carlo Simulation, SCOZA, HRT
Note: The following files were submitted by the author for peer review, but cannot be converted to PDF. You must view these files (e.g. movies) online.	
article_rev.tex	

scholarONE™
Manuscript Central

Molecular Physics, Vol. 00, No. 00, DD Month 200x, 1–18

Liquid-vapour transition of the long range Yukawa fluid.

Jean-Michel Caillol *, Federica Lo Verso †, Elisabeth Schöll-Paschinger ‡, Jean-Jacques Weis * §

* Laboratoire de Physique Théorique, UMR 8627, Bât. 210, Université de Paris-Sud, 91405 Orsay Cedex, France

† Institut für Theoretische Physik II, Heinrich-Heine-Universität Düsseldorf, Universitätsstrasse 1, D-40225 Düsseldorf, Germany

‡ CMS and Fakultät für Physik, Universität Wien, Boltzmanngasse 5, A-1090 Wien, Austria

(*Received 00 Month 200x; In final form 00 Month 200x*)

Two liquid state theories, the self-consistent Ornstein-Zernike equation (SCOZA) and the hierarchical reference theory (HRT) are shown, by comparison with Monte Carlo simulations, to perform extremely well in predicting the liquid-vapour coexistence of the hard core Yukawa (HCY) fluid when the interaction is long range. The long range of the potential is treated in the simulations using both an Ewald sum and hyperspherical boundary conditions. In addition, we present an analytical optimised mean field theory which is exact in the limit of an infinitely long range interaction. The work extends a previous one by Caccamo *et al* [*Phys. Rev. E,* **60**, 5533 (1999)] for short range interactions.

keywords : Yukawa potential, Critical phenomena, Monte Carlo simulations, SCOZA, HRT.
PACS numbers :

1 Introduction

Two liquid state theories are presently available which provide an accurate description of the liquid-vapour transition of simple systems including the critical region. A first one is the so-called self-consistent Ornstein-Zernike approximation (SCOZA) devised initially by Høye and Stell [1, 2] and later adapted for numerical calculations [3–5]. It is based on the assumption that the direct correlation function behaves, to a good approximation, at long range (attractive region of the potential) as the potential with a density and temperature dependent prefactor which is determined by imposing consistency between the energy and compressibility routes to the thermodynamics. The second approach put forward by Parola and Reatto [6], incorporates renormalisation group ideas by gradually taking into account fluctuations of longer and longer wavelengths. It is based on the hierarchical reference theory (HRT) of fluids truncated at lowest order by means of an ORPA-like (optimised random phase approximation) ansatz (see Ref. [7] for review). Both predict non-classical critical exponents [6, 8]. Thermodynamic properties and phase diagrams based on the SCOZA and HRT approaches have been reported for a variety of potentials (limiting ourselves to continuum systems) including the hard core Yukawa (HCY) potential [9–12], the square well potential [13, 14], the Lennard-Jones (LJ) potential [15–18], the Gaussian potential [19], ultrasoft potentials [20], Asakura-Oosawa pair potentials [21, 22], Girifalco potentials [16, 23, 24], binary hard core Yukawa mixtures [25–28], etc.. Most of the comparisons with simulation data are so far restricted to short or medium range

*Corresponding author. Email: Jean-Michel.Caillol@th.u-psud.fr
† Email:federica@thphy.uni-duesseldorf.de
‡ Email:elisabeth.schoell-paschinger@univie.ac.at
§ Email:jean-jacques.weis@th.u-psud.fr

Molecular Physics
ISSN 0026-8976 print/ ISSN 1362-3028 online ©2005 Taylor & Francis Ltd
http://www.tandf.co.uk/journals
DOI: 10.1080/002689700xxxxxxxxxxxx

For Peer Review Only

potentials. The aim of this article is to extend such comparisons to long range interactions. A convenient choice to do this is the HCY potential as the range can be varied from short range appropriate for modelling colloidal suspensions or protein solutions to medium range, where it mimics the familiar LJ potential [10], to long range. For long range interactions we have considered a third approach, an optimised mean field theory (OMF) [29], exact in the Kac limit [30], which can be worked out analytically for the HCY potential (see section 6). A further advantage of the HCY potential is that the repulsive part of the potential which in SCOZA, HRT and OMF is used as a reference potential is a hard sphere potential whose properties are accurately known [31–33]. Last, an approximate analytical solution (mean spherical approximation) is available for the HCY potential [34,35] which drastically reduces the computational efforts of the solution of the SCOZA equations.

For short inverse screening lengths α of the Yukawa potential, $1.8 \leq \alpha\sigma = \alpha^* < 7$ (σ hard sphere diameter), a comparison between SCOZA, HRT and simulation results for the liquid-vapour coexistence curve is available in [10]. In this work we extend the domain of α from $\alpha^* = 1.8$ (where the HCY potential approximates the LJ potential) to $\alpha^* = 0$, the infinite long range potential. With respect to simulations, in this domain the range of the Yukawa potential generally exceeds the dimensions of the simulation box (for typical system sizes of a thousand particles) and some care is necessary to properly treat the long range of the potential. This has been done both by using periodic boundary conditions (b.c.) and performing an Ewald (EW) sum [36] and by using hyperspherical b.c. [37,38].

The remainder of the paper is organised as follows: In section 2 we define the HCY interaction. Section 3 provides a description of the two Monte Carlo (MC) methods used to treat the long range of the Yukawa interaction, Ewald sum and hyperspherical method. After summarising the three considered theories, SCOZA, HRT and OMF in section 4 we compare, in section 5, the numerical results obtained with the different theories for the liquid-vapour coexistence curve and the thermodynamic properties along the coexistence boundary with the simulation results. The conclusions are presented in section 6. An appendix describes some properties of Yukawa charge distributions relevant for elaborating the OMF theory.

2 Model

In our system particles interact by the hard-core Yukawa potential

$$v(r) = \begin{cases} \infty & r \leq \sigma \\ -q^2\alpha^{*2}\dfrac{e^{-\alpha^* r/\sigma}}{r} & r > \sigma \end{cases} . \tag{1}$$

In the limit $\alpha \to 0$ the potential gets infinitely long range and infinitely weak (Kac limit). We define an inverse reduced temperature $\beta^* = 1/T^* = q^2/k_{\mathrm{B}}T\sigma$, where k_{B} is the Boltzmann constant, T the temperature and q has dimension of an electric charge. The reduced density is $\rho^* = \rho\sigma^3$.

3 Simulations.

Numerical simulations of fluids or plasmas involving Yukawa interactions $v(r) \propto \exp(-\alpha r)/r$ can be performed either in a cube of side L with periodic b.c. ($\mathcal{C}_3$) or on the surface of a four dimensional (4D) sphere of centre O and radius R (equation $x^2 + y^2 + z^2 + u^2 = R^2$), the hypersphere $\mathcal{S}_3$ for short. In both geometries the Helmholtz equation $(\Delta - \alpha^2)v(\mathbf{x}) = -\mathbf{4}\pi\delta(\mathbf{x})$ can be solved analytically.

3.1 *Ewald sums.*

In the case of $\mathcal{C}_3$ the solution of the Helmholtz equation can be reexpressed in terms of Ewald sums with good convergence properties [36]. The use of an Ewald potential is of course only necessary when the range of the Yukawa potential exceeds the linear dimensions of the simulation box. Molecular dynamics

For Peer Review Only

simulations of simple models of Yukawa plasmas were performed recently with this method [39, 40]. For the potential model Eq. (1) the Ewald sum for the energy is given by [36]

$$U = -\frac{1}{2}q^2\alpha^{*2}\sum_{i=1}^{N}\sum_{j=1}^{N}\sum_{\mathbf{n}}{}' \Big[\mathrm{erfc}\Big(\eta|\mathbf{r}_{ij}+L\mathbf{n}|+\frac{\alpha}{2\eta}\Big)e^{\alpha|\mathbf{r}_{ij}+L\mathbf{n}|}$$
$$+\mathrm{erfc}\Big(\eta|\mathbf{r}_{ij}+L\mathbf{n}|-\frac{\alpha}{2\eta}\Big)e^{-\alpha|\mathbf{r}_{ij}+L\mathbf{n}|}\Big]\Big/2|\mathbf{r}_{ij}+L\mathbf{n}|$$
$$-\frac{2\pi}{V}q^2\alpha^{*2}\sum_{\mathbf{k}=0}^{\infty}\frac{e^{-(\mathbf{k}^2+\alpha^2)/4\eta^2}}{\mathbf{k}^2+\alpha^2}F(\mathbf{k})F^*(\mathbf{k})+U_{self} \tag{2}$$

where

$$U_{self}/N = -\frac{1}{2}q^2\alpha^{*2}\sum_{\mathbf{n}\neq\mathbf{0}}\Big[\mathrm{erfc}\Big(\eta L|\mathbf{n}|+\frac{\alpha}{2\eta}\Big)e^{\alpha L|\mathbf{n}|}$$
$$+\mathrm{erfc}\Big(\eta L|\mathbf{n}|-\frac{\alpha}{2\eta}\Big)e^{-\alpha L|\mathbf{n}|}\Big]\Big/2L|\mathbf{n}|$$
$$-\frac{2\pi}{V}q^2\alpha^{*2}\sum_{\mathbf{k}=0}^{\infty}\frac{e^{-(\mathbf{k}^2+\alpha^2)/4\eta^2}}{\mathbf{k}^2+\alpha^2}$$
$$+q^2\alpha^{*2}\frac{\eta}{\sqrt{\pi}}e^{-\alpha^2/4\eta^2}-q^2\alpha^{*2}\,\frac{\alpha}{2}\mathrm{erfc}\Big(\frac{\alpha}{2\eta}\Big). \tag{3}$$

and

$$F(\mathbf{k}) = \sum_{i=1}^{N}\exp[i\mathbf{k}\cdot\mathbf{r}_i], \tag{4}$$

In Eq. (2) $\mathbf{r}_{ij} = \mathbf{r}_j - \mathbf{r}_i$, L is the box length, $V = L^3$ the volume and erfc denotes the complementary error function. The prime in the sum over $\mathbf{n} = (n_x, n_y, n_z)$, with n_x,n_y, n_z integers, restricts it to $i \neq j$ for $\mathbf{n} = 0$. The parameter η governs the convergence of the real-space and reciprocal contributions to the energy. With $\eta = 6.5/L$, adopted in our calculations, only terms with $\mathbf{n} = 0$ need to be retained in Eq. (2). The sum in reciprocal space extends over all lattice vectors $\mathbf{k} = 2\pi\mathbf{n}/L$ with $|\mathbf{n}^2| \leq 36$.

3.2 *The hypersphere method for Yukawa interactions.*

In the $\mathcal{S}_3$ geometry the Green's function of the Helmholtz equation for the Yukawa fluid is obtained analytically [37, 38]:

$$v^{\mathcal{S}_3}(\psi) = \frac{1}{R}\frac{\sinh(\omega(\pi-\psi))}{\sin\psi\sinh(\omega\psi)} \quad \text{for} \quad \alpha R \geq 1\ ,$$
$$= \frac{1}{R}\frac{\sin(\omega(\pi-\psi))}{\sin\psi\sin(\omega\psi)} \quad \text{for} \quad \alpha R \leq 1\ ,$$

where $\omega = (|\alpha^2R^2-1|)^{1/2}$. The pair potential $v = -q^2\alpha^{*2}v^{\mathcal{S}_3}(\psi)$ in $\mathcal{S}_3$ is isotropic and depends only on the geodesic length $R\psi$. The geodesic distance between two points $\mathbf{R_1}$ and $\mathbf{R_2}$ of $\mathcal{S}_3$ is given by

$$d_{12} = R\psi_{12} = R\arccos\Big(\frac{\mathbf{R_1}\cdot\mathbf{R_2}}{R^2}\Big)\ . \tag{5}$$

For Peer Review Only

The configurational energy of a system of N Yukawa hard spheres in $\mathcal{S}_3$ is therefore given by

$$V(1,\ldots,N) = \sum_{i<j} v(\psi_{ij}) + \sum_{i<j} v_{\rm HS}^{\mathcal{S}_3}(\psi_{ij}) - \frac{q^2\alpha^{*2}}{2} N V_0 \,. \tag{6}$$

In equation (6) $v_{\rm HS}^{\mathcal{S}_3}(\psi_{ij})$ denotes the hard sphere potential in $\mathcal{S}_3$, i.e.

$$\begin{aligned} v_{\rm HS}^{\mathcal{S}_3}(\psi) &= 0 \quad R\psi > \sigma \\ &= \infty \quad R\psi < \sigma \,. \end{aligned} \tag{7}$$

The presence of the constant V_0 in the r.h.s. of equation (6) accounts for the fact that the energy is defined up to an additive constant. The choice of V_0 is a recurrent problem of simulations in $\mathcal{S}_3$ (see e.g. the discussion in reference [37]). Here we define V_0 by requiring that the self energies in $\mathcal{S}_3$ and the usual Euclidean space $\mathbb{R}^3$ coincide, i.e., $V_0 = \lim_{r\to 0}\left(\exp(-\alpha r)/r - v^{\mathcal{S}_3}(r/R)\right)$ which gives

$$\begin{aligned} V_0 &= -\alpha + \frac{\omega}{R}\cot(\omega\pi) \quad \alpha R < 1 \\ &= -\alpha + \frac{\omega}{R}\coth(\omega\pi) \quad \alpha R > 1 \end{aligned} \tag{8}$$

Recent Monte Carlo simulations of Yukawa plasmas have been performed with this method [38, 41]. Here we apply it to a liquid of attractive Yukawa spheres.

4 Theory

4.1 *SCOZA*

The self-consistent Ornstein-Zernike approximation in its most general formulation is a liquid-state theory that introduces in the relation between the direct correlation function $c(r)$ and the pair potential $v(r)$ one or more state-dependent parameters that are determined by imposing consistency between the different routes to thermodynamics leading to a partial differential equation (PDE) for the unknown parameter(s). The SCOZA originally grew out of the semi-analytic solution of the mean spherical approximation (MSA) for HCY potentials [1, 2, 5] and it is this SCOZA formulation that is considered in the present work. It is based on the Ornstein-Zernike equation supplemented with an MSA-type closure relation

$$\begin{aligned} g(r) &= 0 && \text{for} \quad r \le \sigma \\ c(r) &= c_{\rm HS}(r) + K(\rho,\beta)v(r) && \text{for} \quad r > \sigma. \end{aligned} \tag{9}$$

Here $g(r)$ is the pair distribution function, $c_{\rm HS}(r)$ is the direct correlation function of the hard-core reference system given e.g. in the Waisman parameterisation [34] and $K(\rho,\beta)$ is the state-dependent parameter, that is not given in advance but is determined so that thermodynamic consistency is obtained between the energy and compressibility routes ($\beta = 1/k_{\rm B}T$). The consistency requirement leads to a PDE of the form

$$\frac{\partial}{\partial\beta}\left(\frac{1}{\chi_{\rm red}}\right) = \rho\frac{\partial^2 u}{\partial\rho^2}\,, \tag{10}$$

where $\chi_{\rm red} = \left(1 - \rho\int c(r)d^3r\right)^{-1}$ is the reduced (with respect to the ideal gas) dimensionless isothermal compressibility given by the compressibility route and u is the excess (over ideal gas) internal energy per volume provided by the energy route, i.e. $u = 2\pi\rho^2\int_\sigma^\infty dr r^2 v(r)g(r)$. Once $1/\chi_{\rm red}$ is expressed in terms of

For Peer Review Only

the excess internal energy the PDE eq.(10) can be transformed into a PDE for u

$$B(\rho,u)\frac{\partial u}{\partial \beta} = \rho\frac{\partial^2 u}{\partial \rho^2}. \tag{11}$$

For the general case of an arbitrary attractive tail of the pair interaction the determination of $B(\rho,u)$ must be done fully numerically [14] and requires an enormous amount of computational cost. However, this procedure is not necessary for the fluid considered here: for certain pair potentials, like the hard-core Yukawa potential or hard-core potentials with linear combinations of Yukawa and exponential tails - so called Sogami-Ise fluids, the coefficient $B(\rho,u)$ can be obtained semi-analytically due to the availability of the semi-analytic MSA solution for these potentials. Details of the determination of $B(\rho,u)$ can be found in Ref. [9], [42] and [43]. While the former formulation of SCOZA in Ref. [9] is based on the Laplace transformation route for solving the underlying MSA for hard-core Yukawa fluids, we have used in the present work the reformulation described in Refs. [42] and [43] which is based on the Wertheim-Baxter factorisation method for the solution of the MSA. While both solution methods are equivalent for the potential considered here, the Wertheim-Baxter factorisation method is more flexible and allows a broader applicability of the SCOZA [23, 25].

The PDE is a quasilinear diffusion equation that has been solved numerically via an implicit finite-difference algorithm in the region $(\beta^\star,\rho^\star) \in [0,\beta_f]\times[0,1]$ with suitable initial and boundary conditions (see Ref. [4] for more details). We have chosen a density and temperature grid spacing of $\Delta\rho^\star = 10^{-4}$ and $\Delta\beta^\star = 2\cdot 10^{-4}$. Up to now SCOZA has been applied to a number of discrete [3, 4] and continuum systems [9, 26] and the results showed - when compared with computer simulations - that the theory yields very accurate predictions for the thermodynamic and structural properties throughout the temperature-density plane, even near the phase coexistence and in the critical region. Indeed, SCOZA is one of very few liquid state theories that do not show serious problems in the critical region and even exhibit some form of scaling with non-classical, partly Ising-like critical exponents [8].

4.2 *HRT*

In HRT the pair potential $v(r)$ is divided into a repulsive reference potential part $v_R(r)$ and a longer-ranged attractive part $w(r)$. In the present case the reference system is the hard-sphere fluid, whose thermodynamics and correlations are accurately described by the Carnahan-Starling equation of state [31] and the Verlet-Weis parameterisation of the two-body radial distribution function [32]. The HRT differs from the conventional liquid state approaches in the way the attractive perturbation is dealt with: in order to take into account the effect of fluctuations, $w(r)$ is introduced gradually via a sequence of Q systems whose interaction potential $v_Q(r)$ results from the sum of $v_R(r)$ and a perturbation $w_Q(r)$. The latter term is defined by its Fourier transform $\widetilde{w}_Q(k)$ which coincides with $\widetilde{w}(k)$ for $k > Q$, and is identically vanishing for $k < Q$. As Q evolves from $Q = \infty$ to $Q = 0$, the interaction $v_Q(r) = v_R(r) + w_Q(r)$ goes from the reference part $v_R(r)$ to the full potential $v(r)$. In other words the parameter Q plays the role of an infrared cutoff whose effect consists in depressing fluctuations on length scales larger than $1/Q$: the critical fluctuations are recovered only in the limit $Q \to 0$. The corresponding evolution of thermodynamics and correlations of increasing order can be determined via perturbation theory and is described by an exact hierarchy of integro-differential equations. As mentioned above close to a critical point and at large length scales, this hierarchy becomes equivalent to a formulation of the momentum-space renormalisation group [47]. Unlike current liquid-state theories HRT preserves the correct convexity of the free energy also below the critical temperature, producing flat isotherms in the coexistence region which correspond to infinite compressibility and constant chemical potential. The first equation of the hierarchy gives the evolution of the Helmholtz free energy A_Q of the partially interacting system in terms of its two-body direct correlation function in momentum space $c_Q(k)$ and the full perturbation $\widetilde{w}(k)$:

$$\frac{\partial \mathcal{A}_Q}{\partial Q} = -\frac{Q^2}{4\pi^2}\ln\left(1-\frac{\Phi(Q)}{\mathcal{C}_Q(Q)}\right) \tag{12}$$

For Peer Review Only

where $\Phi(k) = -\widetilde{w}(k)/k_{\rm B}T$. The quantities $\mathcal{A}_Q$, $\mathcal{C}_Q(k)$ are linked to A_Q and $c_Q(k)$ by the relations

$$\mathcal{A}_Q = -\frac{A_Q}{k_{\rm B}TV} + \frac{1}{2}\rho^2\left[\Phi(k{=}0) - \Phi_Q(k{=}0)\right] - \frac{1}{2}\rho\int\frac{d^3\mathbf{k}}{(2\pi)^3}\left[\Phi(k) - \Phi_Q(k)\right] \tag{13}$$

$$\mathcal{C}_Q(k) = c_Q(k) + \Phi(k) - \Phi_Q(k)\,, \tag{14}$$

where V is the volume and ρ the number density. These modified free energy and direct correlation function have been introduced in order to remove the discontinuities which appear in A_Q and $c_Q(k)$ at $Q = 0$ and $k = Q$ respectively as a consequence of the discontinuity of $\widetilde{w}_Q(k)$ at $k = Q$. Indeed, they represent the free energy and direct correlation function of the fully interacting fluid as given by a treatment such that the Fourier components of the interaction with wavelengths larger than $1/Q$ are not really disregarded, but approximately taken into account by mean-field theory. In the $Q \to 0$ limit the modified quantities coincide with the physical ones, once the fluctuations have been fully included. For $Q = \infty$ the definitions in Eqs. (13) and (14) reduce, instead, to the well-known mean-field expressions of the free energy and direct correlation function.

A simple approximation scheme consists in truncating the hierarchy at the first equation, supplementing it with a suitable closure relation based on some ansatz for $\mathcal{C}_Q(k)$. As in previous applications, our form of $\mathcal{C}_Q(k)$ has been inspired by liquid-state theories,

$$\mathcal{C}_Q(k) = \widetilde{c}_{\rm HS}(k) + \lambda_Q\,\Phi(k) + \mathcal{G}_Q(k)\,, \tag{15}$$

where $\widetilde{c}_{\rm HS}(k)$ is the Fourier transform of the direct correlation function of the hard-sphere fluid, and λ_Q, $\mathcal{G}_Q(k)$ are *a priori* unknown functions of the thermodynamic state and of Q. The function $\mathcal{G}_Q(k)$ is determined by the core condition, i.e., the requirement that the radial distribution function $g_Q(r)$ is vanishing for every Q whenever the interparticle separation is less than the hard-sphere diameter σ. Via Eq. (15) we can write the core condition in terms of an integral equation for $c_Q(k)$. λ_Q is adjusted so that $\mathcal{C}_Q(k)$ satisfies the compressibility rule. For each Q-system this constraint gives the reduced compressibility of the fluid as the structure factor evaluated at zero wavevector, and can be expressed in terms of the modified quantities $\mathcal{A}_Q$, $\mathcal{C}_Q(k)$ as

$$\mathcal{C}_Q(k{=}0) = \frac{\partial^2\mathcal{A}_Q}{\partial\rho^2}\,. \tag{16}$$

This equation can be regarded as a consistency condition between the compressibility route and a route in which the thermodynamics is determined from the Helmholtz free energy as obtained from Eq.(12). Here the compressibility rule (16) plays a fundamental role. In fact, when λ_Q in Eq.(15) is determined via Eq.(16) and the resulting expression for $\mathcal{C}_Q(k)$ is used in Eq.(12), one obtains a partial differential equation for $\mathcal{A}_Q$ which reads

$$\frac{\partial\mathcal{A}_Q}{\partial Q} = -\frac{Q^2}{4\pi^2}\,\ln\left[1 - \frac{\Phi(Q)}{\mathcal{A}''_Q\varphi(Q) + \psi(Q)}\right]\,, \tag{17}$$

where we have set $\mathcal{A}''_Q = \partial^2\mathcal{A}_Q/\partial\rho^2$, $\varphi(k) = \Phi(k)/\Phi(0)$ and

$$\psi(k) = \widetilde{c}_{\rm HS}(k) + \mathcal{G}_Q(k) - [\widetilde{c}_{\rm HS}(0) + \mathcal{G}_Q(0)]\varphi(k)\,. \tag{18}$$

Eq.(17) is integrated numerically from $Q = \infty$ down to $Q = 0$. At each integration step, $\mathcal{G}_Q(k)$ is determined by the core condition $g_Q(r) = 0$, $0 < r < \sigma$. This condition acts as an auxiliary equation for determining $\psi(k)$ via Eq.(18).

For this specific work we considered the density interval $\rho^* \in [0, 1]$ to numerically solve the differential equation for the free energy. The spacing of the density grid is $\Delta\rho^* = 10^{-3}$, consequently the error in the

For Peer Review Only

determination of the coexistence densities is of the same order of magnitude. Concerning the boundary conditions: for low density the system behaves as an ideal gas while at $\rho^* = 1$ we assumed the validity of the standard ORPA approximation.

Two remarks are worth mentioning: First, Eq. (15) assumes that the fluid direct correlation function depends linearly on the perturbation $\Phi(k)$. This ansatz is especially appropriate when the perturbation range is much longer than that of the reference part of the interaction, i.e. longer than the particle size. The second remark relates to the implementation of the core condition: the inverse Fourier transform of the function $\mathcal{G}_Q(k)$ has been expanded in a series of Legendre polynomials for $r < \sigma$ and the series has been truncated after a finite number of terms (typically five). The evolution equations for the expansion coefficients were then determined by differentiating with respect to Q the integral equation for $c_Q(k)$, i.e. the core condition, and subsequently projecting it on the polynomials used in the expansion. However, the resulting equations are coupled to the evolution equation 12 for the free energy, and this makes them difficult to handle. Therefore, as described in detail in [21, 22], in the derivative of $c_Q(k)$ with respect to Q the long-wavelength contributions containing the isothermal compressibility of the Q-system were disregarded. Physically this amounts to a decoupling of the short- and the long-range evolutions of the correlations. This approximation, as well as the previous one, are fully justified for long-range perturbations, where the short- and the long-range parts of the correlations are mainly affected by the reference and the perturbation terms respectively, but become more problematic for short-range interactions where the interplay between excluded-volume and cohesion effects is much stronger. However, this effect does not concern the present study.

4.3 *Optimised mean field theory*

We consider, quite generally, a fluid of identical hard spheres of diameter σ with additional isotropic pair interaction $v(r_{ij})$. Since $v(r)$ is an arbitrary function of r for $r \leq \sigma$, one can assume that $v(r)$ has been regularised in the core in such a way that its Fourier transform $\widetilde{v}(k)$ is a well behaved function of k and that $v(0)$ is a finite quantity.

At equilibrium at inverse temperature β and chemical potential μ (grand canonical (GC) ensemble) the pressure p of the fluid is a convex function of $\nu = \beta\mu$ (at fixed β) [48, 49] even before the thermodynamic limit has been taken [48, 49]. As a consequence $\beta p(\nu)$ is continuous, its derivatives with respect to ν exist and it admits a Legendre transform $\beta f(\rho)$ with respect to ν defined as

$$\beta f(\rho) = \sup_{\nu} \{\rho\nu - \beta p(\nu)\} \ . \tag{19}$$

The GC free energy $\beta f(\rho)$ is then a convex function of the density and its Legendre transform with respect to ρ coincides with $\beta p(\nu)$.

It was shown in ref. [29] that in the case of an attractive interaction (i.e. $\widetilde{w}(k) = -\beta\widetilde{v}(k) > 0$ for all q) we have the inequality

$$\begin{aligned} \beta f(\beta,\rho) &\leq \beta f_{\rm MF}(\beta,\rho) \\ \beta f_{\rm MF}(\beta,\rho) &= \beta f_{\rm HS}(\rho) - \frac{1}{2}\rho^2\widetilde{w}(0) + \frac{1}{2}\rho w(0) \ . \end{aligned} \tag{20}$$

Here the subscript mean field (MF) emphasises that $f_{\rm MF}$ is the van der Waals free energy [44]. Note that $\beta f_{\rm MF}[\rho]$ is *a priori* non convex, notably in the two-phase region.

¿From here on we specialise to the Yukawa interaction $w(r) = \beta q^2\alpha^{*2}y(r)$ with $y(r) = \exp(-\alpha r)/r$. Since $y(0) = \infty$, equation (20) does not appear to be very useful. However, it follows from appendix A that we can replace $y(r)$ by the regular function $W_\tau(r)/Q_\tau^2$ where $W_\tau(r)$ is the interaction energy of two spherical distributions $\tau(\mathbf{r})$ of Yukawa charges of effective charge Q_τ. The interaction is regularised in the core but remains unchanged for $r > \sigma$. Since $\widetilde{W}_\tau(k) \geq 0$, Eq. (20) is still valid and will give a non trivial upper bound for the free energy. Similar to what has been done in reference [50] for the Coulomb

For Peer Review Only

interaction we seek a best upper bound for $\beta f(\beta,\rho)$ by minimising the quantity

$$X = \frac{W_\tau(0) - \rho\widetilde{W}_\tau(0)}{Q_\tau^2} \ . \tag{21}$$

To this end we consider variations of X with respect to the charge distribution $\tau(r)$ defined by Eq. (A1) and work out the stationary condition ($\overline{\sigma} = \sigma/2$)

$$\frac{\delta X}{\delta\tau(\mathbf{r})} = 0 \ \text{ for } \ r < \overline{\sigma} \ . \tag{22}$$

First, it follows from equation (A5) that

$$\frac{\delta Q_\tau}{\delta\tau(\mathbf{r})} = \frac{\sinh(\alpha r)}{\alpha r} \ . \tag{23}$$

Second, as a consequence of the convolution relations $V_\tau = \tau * y$ and $W_\tau = \tau * V_\tau = \tau * y * \tau$ one has

$$\frac{\delta W_\tau(\mathbf{r}')}{\delta\tau(\mathbf{r})} = 2V_\tau(|\mathbf{r}' - \mathbf{r}|) \ , \tag{24}$$

and thus

$$\frac{\delta W_\tau(0)}{\delta\tau(\mathbf{r})} = 2V_\tau(r) \ . \tag{25}$$

Finally, since $\widetilde{W}_\tau(0) = 4\pi\alpha^{-2}\widetilde{\tau}^2(0)$, we have

$$\frac{\delta\widetilde{W}_\tau(0)}{\delta\tau(\mathbf{r})} = \frac{8\pi\widetilde{\tau}(0)}{\alpha^2} \ . \tag{26}$$

Collecting results (23), (25) and (26) one gets

$$\begin{aligned}\frac{\delta X}{\delta\tau(\mathbf{r})} = &-\frac{2}{Q_\tau^3}\,\frac{\sinh(\alpha r)}{\alpha r}\,\Big(W_\tau(0) - \rho\widetilde{W}_\tau(0)\Big) \\ &+ \frac{1}{Q_\tau^2}\left(2V_\tau(r) - \frac{8\pi\rho\widetilde{\tau}(0)}{\alpha^2}\right) \ \text{ for } \ r < \overline{\sigma} \ .\end{aligned} \tag{27}$$

Note that we can impose $\widetilde{\tau}(0) = 1$ since, if $\tau(r)$ is solution of the stationary condition (22), then $\lambda\tau(r)$, where $\lambda \neq 0$ is an arbitrary constant, is also a solution (Q_τ is then multiplied by λ but W_τ/Q_τ^2 is left unchanged). Therefore Eq. (22) can be recast in the form

$$V_\tau(r) = \frac{4\pi\rho}{\alpha^2} + \frac{1}{Q_\tau} + \frac{\sinh(\alpha r)}{\alpha r}\Big(W_\tau(0) - \rho\widetilde{W}_\tau(0)\Big) \ . \tag{28}$$

Of course, Eq. (28) is valid only for $r < \overline{\sigma}$. The first contribution in the r.h.s of Eq. (28) is clearly identified with the potential created by a uniform density of Yukawa charges of density ρ while the second contribution stems from a charge discontinuity at $r = \overline{\sigma}$. The solution is therefore of the form $\tau(r) = \rho\Theta(\overline{\sigma}) + K\delta(r - \overline{\sigma})$, where K is a constant determined by the condition $\widetilde{\tau}(0) = 1$, yielding

For Peer Review Only

$$\tau(r) = \rho\Theta(\overline{\sigma}) + \frac{1-\eta}{\pi\sigma^2}\delta(r-\overline{\sigma}) \tag{29}$$

($\eta = \pi\rho\sigma^3/6$ packing fraction). Furthermore, from Eq. (A5) it follows that

$$Q_\tau = 3\eta\frac{\alpha\overline{\sigma}\cosh(\alpha\overline{\sigma}) - \sinh(\alpha\overline{\sigma})}{(\alpha\overline{\sigma})^3} - (1-\eta)\frac{\sinh(\alpha\overline{\sigma})}{\alpha\overline{\sigma}} \tag{30}$$

so that the potential V_τ is seen to be the superposition of two potentials created by spherical surface and volume distributions, the expressions of which are given in appendix A by Eqs. (A13) and (A15), respectively. One finds

$$V_\tau(r) = \frac{24\eta}{\alpha^{*2}} - \frac{2e^{-\alpha^*/2}}{\alpha^{*2}}\left(\eta\alpha^{*2} + 12\eta + 6\eta\alpha^* - \alpha^{*2}\right)\frac{\sinh(\alpha r)}{\alpha r}\ . \tag{31}$$

One can check that V_τ indeed verifies Eq. (28). Finally, the optimised upper bound for the free energy can then be shown to be equal to

$$\beta f(\beta,\rho) \le \beta f_{\rm OMF}(\beta,\rho) \equiv \beta f_{\rm HS}(\rho) + \Delta_{\rm OMF}(\beta,\rho)$$

$$\begin{aligned}\Delta_{\rm OMF} &= \frac{6\beta\eta\alpha^{*3}e^{-\alpha^*}}{\pi}\times \\ &\times\frac{\eta\alpha^{*2} + 6\eta\alpha^* + 12\eta - \alpha^{*2}}{(12\eta - 6\eta\alpha^* - \alpha^{*2} + \alpha^{*2}\eta) - e^{-\alpha^*}(\alpha^{*2} - \alpha^{*2}\eta - 6\eta\alpha^* - 12\eta)} \qquad (32)\\ &= \frac{-72\eta^2}{\pi} - \frac{6\eta(-5-5\eta+\eta^2)}{5\pi}\alpha^{*2} + O(\alpha^{*3})\ . \qquad (33)\end{aligned}$$

An optimised mean field (OMF) theory for the fluid can now be devised by considering the Landau function [48]

$$\mathcal{L}(\beta,\rho,\nu) = \nu\rho - \beta f_{\rm OMF}(\beta,\rho)\ . \tag{34}$$

At given β and ν, the density ρ is the one which minimises the Landau function $\mathcal{L}(\beta,\rho,\nu)$. In the limit $\alpha^* \to 0$, $\Delta_{\rm OMF} = -2\pi\rho^2\beta$ and one thus revovers the free energy of the Kac model for $\alpha = 0$.

5 Results

A comparison between the three theoretical approaches and simulation data for the liquid-vapour coexistence curve is made in Figs. 1 -4 for $\alpha^* = 1.8, 1.0, 0.5$ and 0.1. Values for the densities, internal energies, chemical potentials and Helmholtz free energies along the coexistence curve are presented in Tables 1- 4. These data may be valuable for reference to future approaches.

The simulation results have been obtained with the Gibbs ensemble Monte Carlo (GEMC) method [51,52] using mostly a total of 1000 particles (EW b.c.) and 2000 particles ($\mathcal{S}_3$ b.c.). The number of cycles generated after equilibration varied from 7-40 $\times 10^6$ according to temperature, each cycle comprising with equal probabilities, displacement of the N particles, volume change, or exchange of 500 (EW b.c.) or 1000 particles ($\mathcal{S}_3$ b.c.). Error bars (two standard deviations) were calculated by averaging densities, energies or histograms over blocks of 1 million cycles. Expectedly, uncertainties are largest near the critical temperature where fluctuations of density of the coexisting phases are important and hence convergence slow. Finite size effects additionally affect the critical behaviour, but also influenced to some extent the determination of the coexistence density on the liquid side at least for the smallest value $\alpha^* = 0.1$. Thus, for the $\mathcal{S}_3$ b.c.,

For Peer Review Only

an increase of the number of particles from 1000 to 2000 typically lowered ρ_l^* by about 3%. The opposite trend was observed with the EW b.c. where ρ_l^* increased by $1-2\%$ by an increase of N from 1000 to 1872 (cf. table 4). It is likely that, for $\alpha^* = 0.1$, small finite size effects are still present in both sets of results.

The agreement between HRT, SCOZA and MC simulations turns out to be extremely good over the range of α values considered. Small differences occur only at the highest and lowest values of α. At $\alpha^* = 1.8$ the critical temperature of HRT is slightly below that predicted by SCOZA. Previous work [10] showed, however, that by further increasing the value of α the HRT critical temperature eventually gets higher than that of SCOZA. At $\alpha^* = 0.1$ the coexistence curves, including the critical regions, of SCOZA and OMF are very close (cf. Fig. 4); as the OMF theory is expected to be nearly exact at this small value of α it is very likely that SCOZA becomes exact also in the Kac limit, though no formal proof seems to be available. This is further confirmed by the close agreement between critical parameters of SCOZA and OMF at $\alpha^* = 10^{-5}$ (see table 5). The coexistence curve of HRT is found to be slightly narrower than that of SCOZA though in the near critical region the agreement between the two theories is quite good. As pointed out in ref. [53] the HRT flow cannot be solved conveniently in the Kac limit. Inspection of Fig. 3 shows that the OMF theory rapidly deteriorates with increase of α. Figure 5 compares HRT, SCOZA, OMF and MC simulation results for the internal energy along the coexistence curve at $\alpha^* = 0.5$. The agreement is similar to that for the densities.

The variation with α of the critical temperature and density for SCOZA and HRT, including data of ref. [10] for $\alpha^* > 1.8$, is given in table 5. No attempt has been made to determine critical data in the simulations by fitting data away from the critical point by some power law expression. Because of the finite size effects in the critical region uncertainties of the results would be large and of no use to validate the theoretical predictions. In the GEMC method the order parameter $M = \rho_l - \rho_g$ is believed to have MF behaviour (critical exponent $\beta = 1/2$) in the critical region once the correlation length exceeds the linear dimension L of the simulation box . In fact we find that for $\alpha^* \lesssim 1.0$, M^2 varies linearly over the whole temperature region considered yielding an effective exponent $\beta_{eff} = 1/2$). Such an analysis was not conclusive for $\alpha^* = 1.8$.

6 Conclusion

We have compared the predictions for the liquid-vapour coexistence curve of a long-range Yukawa fluid obtained from advanced theoretical approaches with Gibbs ensemble Monte Carlo simulations. Concerning the simulations care has to be taken when the range of the potential exceeds the length of the simulation box. This was done by performing an Ewald sum in the case of a cubic simulation box and by using hyper-spherical boundary conditions. The theoretical approaches that we applied comprised the self-consistent Ornstein-Zernike approximation (SCOZA), the hierarchical reference theory (HRT), as well as an optimised mean field theory (OMF). While the OMF yields the exact result in the limit of infinite range of the potential, it deteriorates with decreasing interaction range. On the other hand, HRT and SCOZA turn out to be in perfect agreement with simulation results over the whole interaction range considered. This study complements a recent comparison [10] for the case of intermediate and short range Yukawa fluid.

Acknowledgements

This work was supported by a grant through the Programme d'Actions Intégrées AMADEUS under Project Nos. 06648PB and FR 09/2007, by the Hochschuljubiläumsstiftung der Stadt Wien under Project Number 1757/2007 and by the Marie Curie European Network MRTN-CT-2003-504712. Federica Lo Verso thanks Davide Pini, Alberto Parola and Luciano Reatto for helpful discussions.

For Peer Review Only

References

[1] J. S. Høye, G. Stell. *J. Chem. Phys.,* **67**, 439 (1977).
[2] J. S. Høye, G. Stell. *Mol. Phys.,* **52**, 1071 (1984).
[3] R. Dickman, G. Stell. *Phys. Rev. Lett.,* **77**, 996 (1996).
[4] D. Pini, G. Stell, R. Dickman. *Phys. Rev. E,* **57**, 2862 (1998).
[5] D. Pini, G. Stell, J.S. Høye. *Int. J. Thermophys.,* **19**, 1029 (1998).
[6] A. Parola, L. Reatto, *Phys. Rev. A,* **31**, 2417 (1985).
[7] A. Parola, L. Reatto. *Adv. Phys.,* **44**, 211 (1995).
[8] J. S. Høye, D. Pini, G. Stell *Physica A,* **279**, 213 (2000).
[9] D. Pini, G. Stell, N. B. Wilding. *Mol. Phys.,* **95**, 483 (1998).
[10] C. Caccamo, G. Pellicane, D. Costa, D. Pini, G. Stell *Phys. Rev. E,* **60**, 5533 (1999).
[11] D. Pini, Ge Jialin, A. Parola, L. Reatto. *Chem. Phys. Lett.,* **327**, 209 (2000).
[12] D. Pini, A. Parola, L. Reatto. *J. Phys.: Condens. Matter,* **18**, S2305 (2006).
[13] A. Reiner, G. Kahl. *J. Chem. Phys.,* **117**, 4925 (2002).
[14] E. Schöll-Paschinger, A. L. Benavides, R. Castañeda-Priego. *J. Chem. Phys.,* **123**, 234513 (2005).
[15] A. Meroni, A. Parola, L. Reatto. *Phys. Rev. A,* **42**, 6104 (1990).
[16] M. Tau, A. Parola, D. Pini, L. Reatto. *Phys. Rev. E,* **52**, 2644 (1995).
[17] E. Schöll-Paschinger, A. Reiner. *J. Chem. Phys.,* **125**, 164503 (2006).
[18] J. S. Høye, A. Reiner. *J. Chem. Phys.,* **125**, 104503 (2006).
[19] B. M. Mladek, G. Kahl, M. Neumann. *J. Chem. Phys.,* **124**, 064503 (2006).
[20] F. Lo Verso, M. Tau, L. Reatto. *J. Phys.: Condens.Matter* **15**, 1505 (2003).
[21] F. Lo Verso, D. Pini, L. Reatto. *J. Phys.: Condens. Matter* **17**, 771 (2005).
[22] F. Lo Verso, R. L. C. Vink, D. Pini, L. Reatto. *Phys. Rev. E* **73**, 61407 (2006).
[23] E. Schöll-Paschinger, G. Kahl. *Europhys. Letters,* **63**, 538 (2003).
[24] D. Costa, G. Pellicane, C. Caccamo, E. Schöll-Paschinger, G. Kahl *Phys. Rev. E* **68**, 021104 (2003).
[25] E. Schöll-Paschinger, G. Kahl. *J. Chem. Phys.,* **118**, 7414 (2003).
[26] E. Schöll-Paschinger, D. Levesque, J.-J. Weis, G. Kahl. *J. Chem. Phys.,* **122**, 024507 (2005).
[27] E. Schöll-Paschinger, G. Kahl. *J. Chem. Phys.,* **123**, 134508 (2005).
[28] D. Pini, M. Tau, A. Parola, L. Reatto. *Phys. Rev. E,* **67**, 046116 (2003).
[29] J.-M. Caillol. *Mol. Phys.,* **101**, 1617 (2003).
[30] M. Kac, G.E. Uhlenbeck, P.C. Hemmer, *J. Math, Phys.,* **4**, 216 (1963).
[31] N. F. Carnahan, K.E. Starling *J. Chem. Phys.,***51**, 635 (1969).
[32] L. Verlet, J. J. Weis. *Phys. Rev. A,***5**, 939 (1972).
[33] D. Henderson E. W. Grundke. *J. Chem. Phys.,* **63**, 601 (1975).
[34] E. Waisman. *Mol. Phys.,* **25**, 45 (1973).
[35] L. Blum, J.S. Høye. *J. Stat. Phys.,* **19**, 317 (1978).
[36] G. Salin, J.-M. Caillol. *J. Chem. Phys.,* **113**, 10459 (2000).
[37] J.-M. Caillol, D. Gilles. *J. Stat. Phys.,* **100**, 905 (2000).
[38] J.-M. Caillol, D. Gilles. *J. Stat. Phys.,* **100**, 933 (2000).
[39] G. Salin, J.-M. Caillol. *Phys. Rev. Lett.,* **88**, 65002-1-4 (2002).
[40] G. Salin, J.-M. Caillol. *Phys. of Plasmas,* **10**, 1220 (2003).
[41] J.-M. Caillol, D. Gilles. *J. Phys. A: Math. Gen.,* **36**, 6343 (2003).
[42] G. Kahl, E. Schöll-Paschinger, G. Stell. *J. Phys. Condens. Matter,* **14**, 9153 (2002).
[43] E. Schöll-Paschinger. *J. Chem. Phys.,* **120**, 11698(2004).
[44] J.-P. Hansen, I.R. McDonald. *Theory of Simple Liquids* Academic Press, London (1986).
[45] See, for instance, K. G. Wilson, J. B. Kogut *Phys. Rep. C* 12, 75 (1974).
[46] See, for instance, M. E. Fisher *Critical Phenomena*, Lecture Notes in Physics, Vol. **186**, F. J. W. Hahne (Ed.), Springer, Berlin, (1982).
[47] F. Nicoll, T. S. Chang. *Phys. Lett.,* **62A**, 287 (1977).
[48] N. Goldenfeld. *Lectures on Phase Transitions and the Renormalization Group* Addison-Wesley (1992).
[49] J.-M. Caillol. *J. Phys. A : Math. Gen.,* **35**, 4189 (2002).
[50] J.-M. Caillol. *J. Stat. Phys.,* **115**, 1461 (2004).
[51] A.Z. Panagiotopoulos. *Mol. Phys.,* **61**, 813 (1987).
[52] D. Frenkel, B. Smit. *Understanding Molecular Simulation* Academic Press, London (1996).
[53] J.-M. Caillol. *Mol. Phys.,* **104**, 1931 (2006).
[54] Y. Rosenfeld. 1993, *J. Chem. Phys.,* **98**, 8126 (1993).
[55] Y. Rosenfeld. *Phys. Rev. E,* **47**, 2676 (1993).
[56] Y. Rosenfeld. *Mol. Phys.,* **88**, 1357 (1996).
[57] Y. Rosenfeld, G. Chabrier. *J. Stat. Phys.,* **98**, 283 (1997).

For Peer Review Only

Table 1. Coexistence densities, internal energy U, excess chemical potential μ and Helmholtz free energy A at coexistence for $\alpha^* = 1.8$. A^{ref} is the Carnahan-Starling HS free energy [31].

T^*		ρ_v^*	ρ_l^*	$(U/NkT)_v$	$(U/NkT)_l$	μ/kT	$(\Delta a)_v^{\mathrm{a}}$	$(\Delta a)_l^{\mathrm{b}}$
	SCOZA	0.174	0.464	-1.055	-2.650	-2.737		
0.635	HRT	0.181	0.458	-1.106	-2.607		0.963	2.521
	MC-EW	0.175(10)	0.430(15)	-1.06(4)	-2.43(3)	-2.74(1)		
	SCOZA	0.161	0.485	-0.982	-2.770	-2.765		
0.63	HRT	0.166	0.477	-1.030	-2.735		0.890	2.657
	MC-EW	0.171(8)	0.470(15)	-1.05(2)	-2.67(2)	-2.76(1)		
	SCOZA	0.138	0.515	-0.862	-2.996	-2.825		
0.62	HRT	0.142	0.509	-0.901	-2.967		0.774	2.900
	MC-EW	0.149(5)	0.501(4)	-0.94(2)	-2.92(2)	-2.83(1)		
	SCOZA	0.105	0.565	-0.686	-3.407	-2.953		
0.60	HRT	0.108	0.560	-0.724	-3.386		0.609	3.333
	MC-EW	0.109(2)	0.553(4)	-0.73(1)	-3.34(2)	-2.96(1)		
	SCOZA	0.082	0.606	-0.556	-3.803	-3.094		
0.58	HRT	0.083	0.602	-0.578	-3.787		0.486	3.741
	MC-EW	0.083(2)	0.594(4)	-0.58(1)	-3.74(2)	-3.10(1)		
	SCOZA	0.063	0.643	-0.452	-4.204	-3.251		
0.56	HRT	0.065	0.640	-0.490	-4.192		0.396	4.155
	MC-EW	0.063(2)	0.631(4)	-0.46(1)	-4.13(3)	-3.25(3)		
	SCOZA	0.049	0.676	-0.367	-4.614	-3.424		
0.54	HRT	0.050	0.674	-0.390	-4.606		0.317	4.573
	MC-EW	0.050(2)	0.670(4)	-0.39(1)	-4.57(2)	-3.47(8)		
	SCOZA	0.0284	0.738	-0.235	-5.503	-3.834		
0.50	HRT	0.029	0.736	-0.258	-5.500		0.201	5.469
	MC-EW	0.029(2)	0.733(4)	-0.25(1)	-5.47(3)	-3.76(10)		

[a] $(\Delta a)_v = \frac{1}{NkT}(A - A^{ref})_v$

[b] $(\Delta a)_l = \frac{1}{NkT}(A - A^{ref})_l$

Appendix A: Some properties of Yukawa charge distributions

The electrostatics of Yukawa charge distributions is similar to, but not identical with the electrostatics of usual Coulomb charge distributions. In this appendix we extend previous results obtained for special forms of spherical distributions of Yukawa charges [37,54–57] to a general spherical distribution $\tau(r)$ which satisfies:

$$\begin{aligned} \tau(r) &= 0 \ \text{ for } \ r > \overline{\sigma} \equiv \sigma/2 \ , \\ \tau(r) &> 0 \ \text{ for } \ 0 \le r \le \overline{\sigma} \equiv \sigma/2 \end{aligned} \tag{A1}$$

We denote by $y(r)$ the Yukawa potential created by a unit point charge. We have $y(r) = \exp(-\alpha r)/r$ and for its Fourier transform $\widetilde{y}(k) = 4\pi/(\alpha^2 + k^2)$. The Yukawa potential $V_\tau \equiv \tau * y$ created by this distribution at point $\mathbf{R}$ is given by the convolution of τ and y

$$\begin{aligned} V_\tau(R) &= \int_0^{\overline{\sigma}} dr \ 4\pi r^2 \tau(r) I(R,r) \ , \\ I(R,r) &= \int \frac{d\Omega_{\mathbf{r}}}{4\pi} \ \frac{\exp(-\alpha|\mathbf{R}-\mathbf{r})|)}{|\mathbf{R}-\mathbf{r}|} \ , \end{aligned} \tag{A2}$$

where $d\Omega_{\mathbf{r}}$ denotes the infinitesimal spherical angle about vector $\mathbf{r}$. The integral $I(R,r)$ reads [37,54–57]

$$I(R,r) = \frac{\sinh(\alpha r)}{\alpha r} \frac{\exp(-\alpha R)}{R} \ \text{ for } \ R > r \ ,$$

For Peer Review Only

Table 2. Same as table 1 but for $\alpha^* = 1.0$

T^*		ρ_v^*	ρ_l^*	$(U/NkT)_v$	$(U/NkT)_l$	μ/kT	$(\Delta a)_v^{\mathrm{a}}$	$(\Delta a)_l^{\mathrm{b}}$
	SCOZA	0.174	0.396	-0.987	-2.209	-2.773		
0.905	HRT	0.176	0.393	-1.000	-2.195		0.955	2.169
	MC-EW	0.183(2)	0.395(10)	-1.025(50)	-2.19(5)	-2.77(1)		
	SCOZA	0.135	0.450	-0.788	-2.583	-2.864		
0.88	HRT	0.136	0.448	-0.767	-2.477		0.758	2.557
	MC-EW	0.135(2)	0.439(5)	-0.78(2)	-2.52(2)	-2.87(1)		
	SCOZA	0.112	0.484	-0.676	-2.852	-2.944		
0.86	HRT	0.114	0.482	-0.687	-2.842		0.650	2.825
	MC-EW	0.112(2)	0.474(4)	-0.67(1)	-2.79(2)	-2.95(1)		
	SCOZA	0.095	0.514	-0.586	-3.107	-3.028		
0.84	HRT	0.096	0.512	-0.593	-3.098		0.561	3.083
	MC-EW	0.096(2)	0.508(5)	-0.59(2)	-3.07(3)	-3.04(2)		
	SCOZA	0.0806	0.541	-0.511	-3.360	-3.119		
0.82	HRT	0.081	0.540	-0.513	-3.353		0.485	3.341
	MC-EW	0.085(3)	0.543(6)	-0.54(2)	-3.37(3)	-3.11(2)		
	SCOZA	0.0685	0.567	-0.446	-3.615	-3.216		
0.80	HRT	0.069	0.566	-0.451	-3.610		0.424	3.600
	MC-EW	0.070(2)	0.564(4)	-0.447(15)	-3.60(3)	-3.21(1)		
	SCOZA	0.058	0.591	-0.389	-3.873	-3.321		
0.78	HRT	0.059	0.590	-0.401	-3.868		0.372	3.859
	MC-EW	0.062(2)	0.594(6)	-0.420(15)	-3.89(3)	-3.30(2)		
	SCOZA	0.049	0.614	-0.339	-4.140	-3.434		
0.76	HRT	0.050	0.613	-0.353	-4.133		0.324	4.124
	MC-EW	0.050(2)	0.612(3)	-0.344(5)	-4.120(15)	-3.43(1)		
	SCOZA	0.041	0.636	-0.294	-4.413	-3.557		
0.74	HRT	0.042	0.635	-0.304	-4.407		0.280	4.398
	MC-EW	0.042(2)	0.634(4)	-0.30(1)	-4.440(25)	-3.55(1)		

[a] $(\Delta a)_v = \frac{1}{NkT}(A - A^{ref})_v$

[b] $(\Delta a)_l = \frac{1}{NkT}(A - A^{ref})_l$

$$= \frac{\sinh(\alpha R)}{\alpha R}\frac{\exp(-\alpha r)}{r} \quad \text{for} \quad r > R\,. \tag{A3}$$

The potential $V_\tau(R)$ for $R < \overline{\sigma}$ is not particularly useful but outside the sphere (i.e. for $R > \overline{\sigma}$) one infers from equations (A2) and (A3) the remarkable result

$$V_\tau(R) = Q_\tau \frac{\exp(-\alpha R)}{R}\,, \tag{A4}$$

$$Q_\tau = \int_0^{\overline{\sigma}} dr\; 4\pi r^2 \tau(r) \frac{\sinh(\alpha r)}{\alpha r}\,. \tag{A5}$$

As in the case of the Coulomb potential, the potential outside the spherical distribution of charge $y(r)$ is still a Yukawa potential with the same screening parameter α but with a different charge Q_τ. Since $\sinh(x)/x > 0$ the effective charge Q_τ is larger than the bare charge $\widetilde{\tau}(0)$ of the distribution. Of course in the limit $\alpha \to 0$ one has $Q_\tau \to 1$ and Gauss law is recovered.

We now prove the theorem

$$-\frac{V_\tau(R)}{Q_\tau} + y(R) \geq 0 \;\; \forall R\,. \tag{A6}$$

For $R > \overline{\sigma}$ it is obvious; for $R < \overline{\sigma}$ we note that from the expression (A5) of Q_τ and from equation (A2)

For Peer Review Only

Table 3. Same as table 1 but for $\alpha^* = 0.5$

T^*		ρ_v^*	ρ_l^*	$(U/NkT)_v$	$(U/NkT)_l$	μ/kT	$(\Delta a)_v^{\mathrm{a}}$	$(\Delta a)_l^{\mathrm{b}}$
	SCOZA	0.164	0.367	-0.923	-2.063	-2.824		
1.045	HRT	0.163	0.371	-0.916	-2.086		0.908	2.082
	MC-EW	0.169(8)	0.355(8)	-0.93(3)	-1.99(2)	-2.82(1)		
	MC-S3	0.182(5)	0.384(3)	-1.02(3)	-2.15(3)			
	SCOZA	0.157	0.377	-0.885	-2.131	-2.839		
1.04	HRT	0.156	0.381	-0.881	-2.153		0.873	2.149
	MC-EW	0.160(8)	0.370(8)	-0.89(4)	-2.05(4)	-2.84(1)		
	MC-S3	0.165(6)	0.384(6)	-0.93(3)	-2.172(22)			
	SCOZA	0.133	0.412	-0.764	-2.377	-2.899		
1.02	HRT	0.132	0.415	-0.760	-2.394		0.752	2.390
	MC-EW	0.130(6)	0.400(6)	-0.75(2)	-2.31(4)	-2.90(1)		
	MC-S3	0.133(2)	0.415(3)	-0.77(1)	-2.39(2)			
	SCOZA	0.114	0.442	-0.670	-2.602	-2.962		
1.00	HRT	0.114	0.445	-0.670	-2.620		0.662	2.617
	MC-EW	0.118(4)	0.439(4)	-0.689(15)	-2.58(2)	-2.96(1)		
	MC-S3	0.111(1)	0.441(2)	-0.655(50)	-2.60(1)			
	SCOZA	0.099	0.469	-0.594	-2.817	-3.030		
0.98	HRT	0.099	0.470	-0.594	-2.826		0.587	2.824
	MC-EW	0.103(4)	0.467(4)	-0.62(1)	-2.74(2)	-3.02(1)		
	MC-S3	0.095(1)	0.466(2)	-0.573(54)	-2.800(15)			
	SCOZA	0.086	0.493	-0.528	-3.028	-3.101		
0.96	HRT	0.086	0.494	-0.527	-3.035		0.520	3.032
	MC-EW	0.085(4)	0.485(4)	-0.52(1)	-2.99(1)	-3.11(1)		
	MC-S3	0.0846(11)	0.494(3)	-0.521(7)	-3.037(15)			
	SCOZA	0.075	0.516	-0.471	-3.239	-3.178		
0.94	HRT	0.076	0.516	-0.476	-3.240		0.469	3.238
	MC-EW	0.076(2)	0.512(2)	-0.468(5)	-3.21(1)	-3.17(2)		
	MC-S3	0.072(1)	0.509(2)	-0.442(4)	-3.20(1)			
	SCOZA	0.0656	0.538	-0.420	-3.451	-3.259		
0.92	HRT	0.066	0.537	-0.422	-3.447		0.417	3.446
	MC-EW	0.068(2)	0.539(3)	-0.43(1)	-3.46(2)	-3.27(3)		
	MC-S3	0.0678(13)	0.547(3)	-0.437(8)	-3.52(2)			
	SCOZA	0.0572	0.559	-0.374	-3.667	-3.346		
0.90	HRT	0.058	0.557	-0.380	-3.658		0.374	3.656
	MC-EW	0.058(2)	0.556(3)	-0.375(10)	-3.64(2)	-3.34(1)		
	MC-S3	0.058(1)	0.566(3)	-0.382(7)	-3.72(2)			

[a] $(\Delta a)_v = \frac{1}{NkT}(A - A^{ref})_v$

[b] $(\Delta a)_l = \frac{1}{NkT}(A - A^{ref})_l$

it follows that

$$V_\tau(R) - Q_\tau y(R) = \int_R^{\overline{\sigma}} dr\ 4\pi r^2 \tau(r) \frac{1}{\alpha r R} Z(r)\ , \tag{A7}$$

where $Z(r) = e^{-\alpha r}\sinh(\alpha R) - \sinh(\alpha r)e^{-\alpha R}$. Since $Z(r)$ is a decreasing function of r and $Z(R) = 0$ we have $Z(r) \leq 0$ from which inequality (A6) follows (note that $\tau(r)$ must be positive). For a sufficiently regular distribution $\tau(r)$, the potential $V_\tau(R)$ is a bounded smooth function for $R < \overline{\sigma}$, in particular $V_\tau(R = 0)$ is finite in general (see examples at the end of the appendix).

Clearly the Fourier transform $\widetilde{V}_\tau(k) = 4\pi\widetilde{\tau}(k)/(\alpha^2 + k^2)$ has not a definite sign in general although $\widetilde{V}_\tau(0) = 4\pi\widetilde{\tau}(0)\alpha^{-2} > 0$.

The interaction $W_\tau(1, 2)$ of two identical spherical distributions of Yukawa charges centred at points $\mathbf{R_1}$ and $\mathbf{R_2}$ is now given by (with obvious notations)

For Peer Review Only

Table 4. Same as table 1 but for $\alpha^* = 0.1$

T^*		ρ_v^*	ρ_l^*	$(U/NkT)_v$	$(U/NkT)_l$	μ/kT	$(\Delta a)_v^{\mathrm{a}}$	$(\Delta a)_l^{\mathrm{b}}$
	SCOZA	0.158	0.357	-0.900	-2.030	-2.863		
1.10	HRT	0.161	0.353	-0.916	-2.010		-0.916	-2.010
	MC-EW	0.17(1)	0.340(15)	-0.96(2)	-1.96(5)	-2.86(2)		
	MC-S3	0.167(5)	0.361(5)	-0.93(3)	-2.05(2)			
	SCOZA	0.145	0.375	-0.834	-2.155	-2.891		
	HRT	0.148	0.371	-0.850	-2.132		-0.850	-2.131
1.09	MC-EW	0.145(10)	0.360(15)	-0.82(1)	-2.05(1)	-2.89(1)		
	MC-EW1	0.145(4)	0.362(3)	-0.82(2)	-2.07(2)	-2.895(5)		
	MC-S3	0.160(6)	0.392(3)	-0.92(2)	-2.25(2)			
	SCOZA	0.134	0.391	-0.778	-2.270	-2.918		
1.08	HRT	0.138	0.387	-0.800	-2.244		-0.800	-2.244
	MC-EW	0.136(5)	0.380(5)	-0.79(2)	-2.21(2)	-2.92(2)		
	MC-S3	0.1384(24)	0.395(3)	-0.8018(15)	-2.29(2)			
	SCOZA	0.124	0.406	-0.730	-2.379	-2.947		
	HRT	0.128	0.401	-0.749	-2.347		-0.749	-2.347
1.07	MC-EW	0.126(2)	0.393(3)	-0.73(1)	-2.32(2)	-2.95(1)		
	MC-EW1	0.127(2)	0.399(3)	-0.74(1)	-2.34(2)	-2.95(1)		
	MC-S3	0.1260(15)	0.4103(21)	-0.737(8)	-2.402(13)			
	SCOZA	0.116	0.420	-0.686	-2.484	-2.977		
1.06	HRT	0.120	0.415	-0.708	-2.452		-0.708	-2.452
	MC-EW	0.121(4)	0.416(4)	-0.716(15)	-2.46(2)	-2.97(1)		
	MC-S3	0.118(2)	0.423(3)	-0.697(11)	-2.544(15)			
	SCOZA	0.1082	0.434	-0.647	-2.587	-3.007		
	HRT	0.112	0.427	-0.667	-2.547		-0.667	-2.547
1.05	MC-EW	0.109(2)	0.425(3)	-0.65(1)	-2.54(2)	-3.000(15)		
	MC-EW1	0.113(2)	0.433(3)	-0.68(1)	-2.59(2)	-3.00(1)		
	MC-S3	0.111(2)	0.442(2)	-0.660(7)	-2.63(2)			
	SCOZA	0.101	0.446	-0.610	-2.689	-3.038		
1.04	HRT	0.107	0.439	-0.638	-2.644		-0.638	-2.644
	MC-EW	0.102(1)	0.439(2)	-0.641(5)	-2.64(1)	-3.04(1)		
	MC-S3	0.1047(13)	0.456(3)	-0.630(9)	-2.75(2)			
	SCOZA	0.089	0.470	-0.546	-2.887	-3.103		
1.02	HRT	0.093	0.462	-0.571	-2.837		-0.570	-2.837
	MC-EW	0.091(1)	0.466(2)	-0.555(5)	-2.86(1)	-3.10(1)		
	MC-S3	0.091(1)	0.479(2)	-0.558(6)	-2.94(1)			
	SCOZA	0.078	0.493	-0.489	-3.085	-3.173		
	HRT	0.083	0.483	-0.519	-3.026		-0.519	-3.026
1.00	MC-EW	0.077(3)	0.483(5)	-0.48(1)	-3.028(25)	-3.17(1)		
	MC-EW1	0.078(2)	0.487(5)	-0.484(14)	-3.05(3)	-3.185(15)		
	MC-S3	0.079(1)	0.499(2)	-0.492(6)	-3.126(13)			
	SCOZA	0.0572	0.559	-0.374	-3.667	-3.346		
0.98	HRT	0.074	0.503	-0.472	-3.215		-0.472	-3.215
	MC-EW	0.057(1)	0.539(3)	-0.373(6)	-3.55(2)	-3.35(3)		

[a] $(\Delta a)_v = \frac{1}{NkT}(A - A^{ref})_v$

[b] $(\Delta a)_l = \frac{1}{NkT}(A - A^{ref})_l$

For Peer Review Only

$$W_\tau(1,2) = \int d1'\, d2'\, \tau(1,1')\, y(1',2')\, \tau(2,2')$$
$$= \int d1'\, V_\tau(1,1')\, \tau(1',2)\ . \tag{A8}$$

Also in this case Gauss theorem generalises easily. Indeed, for the case where the two distributions do not

Table 5. Critical parameters. Results based on the Carnahan-Starling hard sphere free energy [31] for the reference system.

α^*		T_c^*	ρ_c^*
0.0	OMF	1.13194	0.24913
10^{-5}	SCOZA	1.1319	0.2491
0.1	SCOZA	1.1294	0.2495
	HRT	1.129	0.250
	OMF	1.13108	0.24915
0.5	SCOZA	1.0718	0.2586
	HRT	1.073	0.260
1.0	SCOZA	0.9264	0.2793
	HRT	0.925	0.279
1.8	SCOZA	0.6527	0.3145
	HRT	0.650	0.314
4.0[a]	SCOZA	0.173	0.3895
	HRT	0.175	0.394
7.0[a]	SCOZA	0.0187	0.4575
	HRT	0.019	0.424

[a] from ref. [10]. Due to a different definition, the temperatures of ref. [10] must be multiplied by the factor α^{*2}/e^{α^*}.

overlap, i.e. $R = |\mathbf{R_2} - \mathbf{R_1}| > \sigma$, $V_\tau(1,1')$ can be replaced by $Q_\tau y(1,1')$ in equation (A8) and thus

$$W_\tau(R) = Q_\tau^2\, y(R) \;\text{ for } R > \sigma\ . \tag{A9}$$

Note that the Fourier transform $\widetilde{W}_\tau(k) = \widetilde{\tau}^2(k)\,\widetilde{y}(k) \geq 0$ is positive definite contrary to $\widetilde{V}_\tau(k)$.

In addition, we have the theorem

$$-\frac{W_\tau(R)}{Q_\tau^2} + y(R) \geq 0 \;\; \forall R\ . \tag{A10}$$

The proof is trivial :

$$\begin{aligned} W_\tau(1,2) &= \int d1'\ \tau(1,1')V_\tau(1',2) \\ &\leq Q_\tau \int d1'\ \tau(1,1')\ y(1',2) \equiv Q_\tau V_\tau(1,2) \\ &\leq Q_\tau^2\ y(1,2)\ . \end{aligned} \tag{A11}$$

The function $W_\tau(r)$ is in general bounded in the core and in particular $W_\tau(0)$ is finite. This charge smearing process provides an easy way to regularise the Yukawa potential $y(r)$ in the core which preserves the positivity of the interaction.

Finally, we give explicit expressions for Q_τ, V_τ for $r < \overline{\sigma}$, and the value $W_\tau(0)$ in simple cases relevant for Sect. 4.3 . Thus for a surface distribution

$$\tau_\sigma(r) = \frac{1}{\pi\sigma^2}\delta(r - \overline{\sigma})\ , \tag{A12}$$

For Peer Review Only

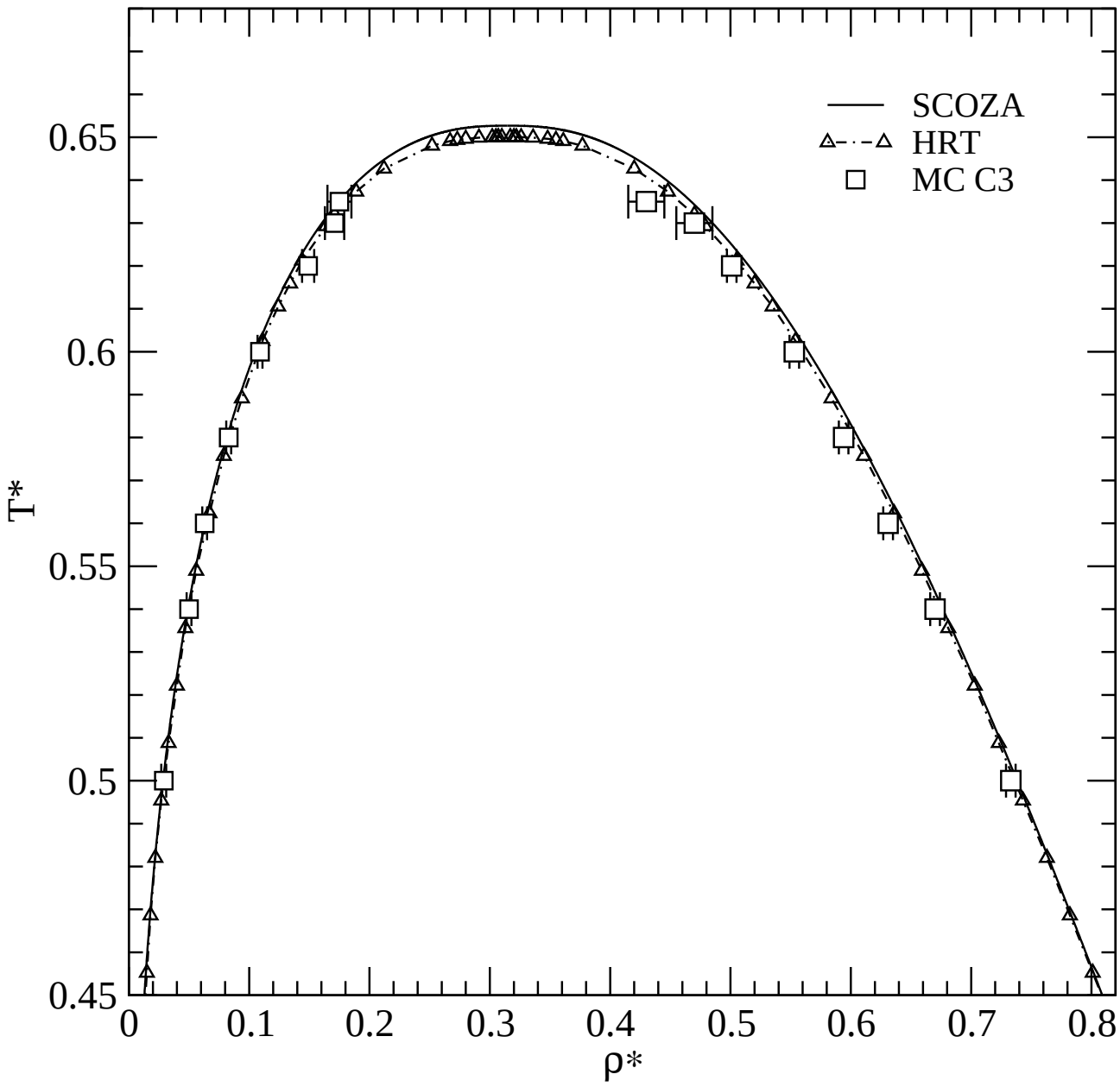

Figure 1. Liquid-vapour coexistence curve of the HCY fluid for $\alpha^* = 1.8$ from SCOZA and HRT. The simulation results (open squares) are for the cubic system with EW sums ($N = 1000$).

one finds

$$
\begin{aligned}
Q_{\tau_\sigma} &= \frac{\sinh(\alpha\overline{\sigma})}{\overline{\sigma}} \\
V_{\tau_\sigma}(r) &= \frac{\exp(-\alpha\overline{\sigma})}{\overline{\sigma}} \frac{\sinh(\alpha r)}{\alpha r} \quad \text{for } r < \overline{\sigma} \\
W_{\tau_\sigma}(0) &= Q_{\tau_\sigma} \frac{\exp(-\alpha\overline{\sigma})}{\overline{\sigma}} \ .
\end{aligned} \tag{A13}
$$

For a volume distribution

$$
\tau_\rho(r) = \frac{6}{\pi\sigma^3}\Theta(\overline{\sigma} - r) \ , \tag{A14}
$$

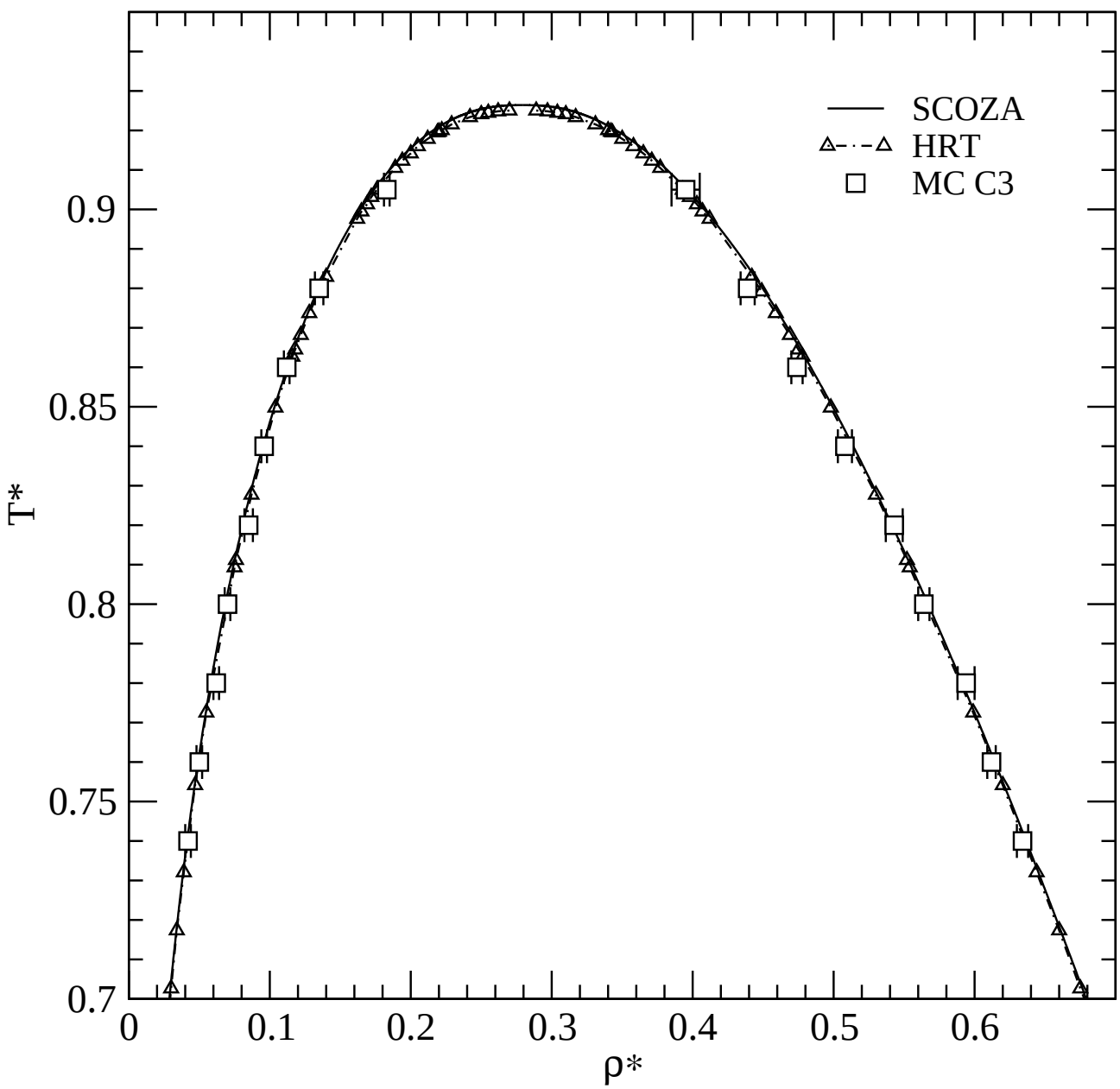

Figure 2. Liquid-vapour coexistence curve of the HCY fluid for $\alpha^* = 1.0$ from SCOZA and HRT. The simulation results (open squares) are for the cubic system with EW sums ($N = 1000$).

(Θ step function) one has

$$Q_{\tau_\rho} = \frac{3}{(\alpha\overline{\sigma})^3}\left(\alpha\overline{\sigma}\cosh(\alpha\overline{\sigma}) - \sinh(\alpha\overline{\sigma})\right)$$

$$V_{\tau_\rho}(r) = \frac{3}{\alpha^2\overline{\sigma}^3}\left(1 - (1+\alpha\overline{\sigma})\exp\left(-\alpha\overline{\sigma}\right)\frac{\sinh\left(\alpha r\right)}{\alpha r}\right) \quad \text{for } r < \overline{\sigma}$$

$$W_{\tau_\rho}(0) = \frac{2}{\alpha^2\overline{\sigma}^3}\left(1 - (1+\alpha\overline{\sigma})\exp\left(-\alpha\overline{\sigma}\right)Q_{\tau_\rho}\right) \ . \tag{A15}$$

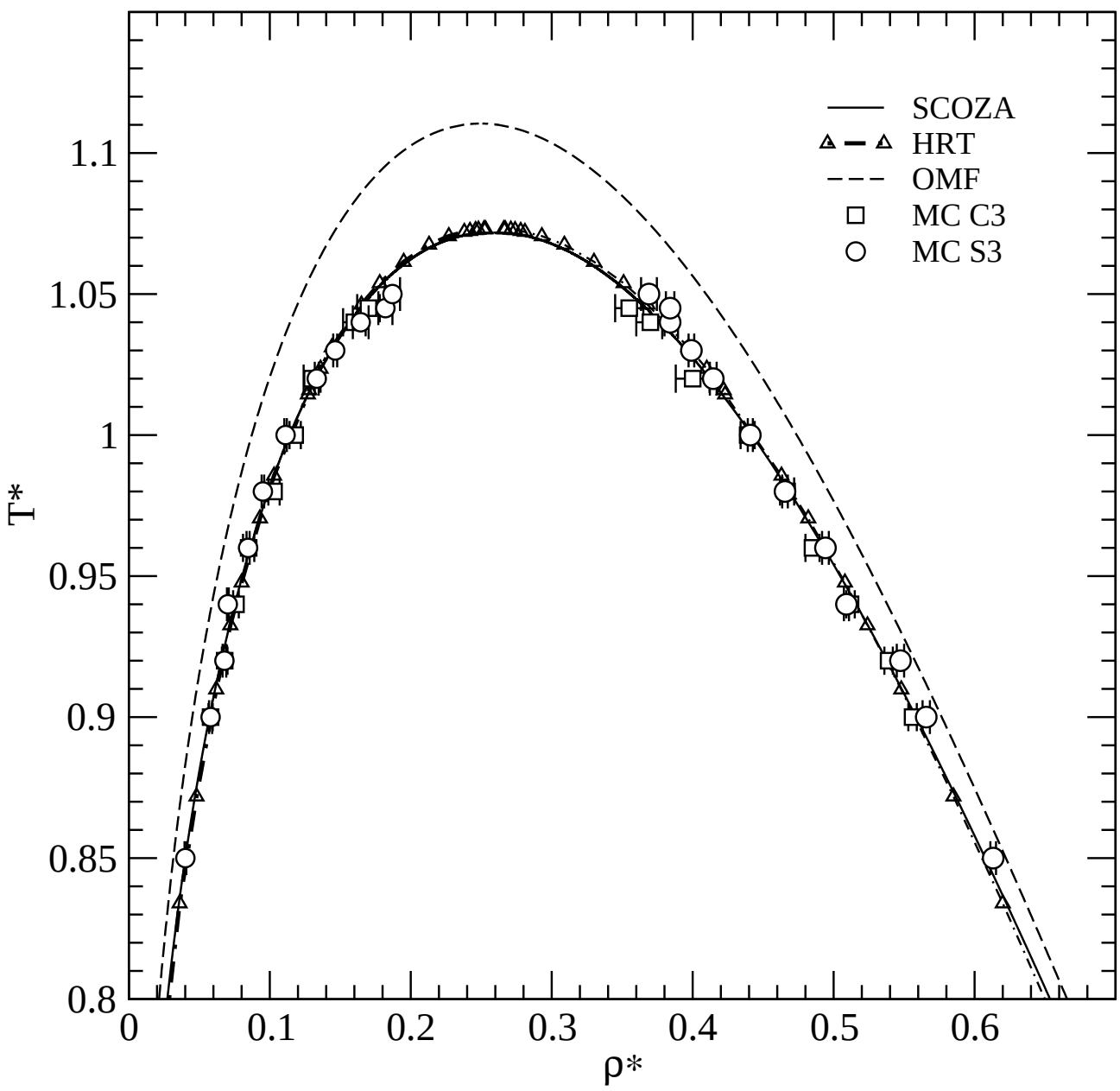

Figure 3. Liquid-vapour coexistence curve of the HCY fluid for $\alpha^* = 0.5$ from SCOZA, HRT and OMF. Open squares: simulation results for the cubic system with EW sums ($N = 1000$); open circles: hypersphere calculations ($N = 2000$).

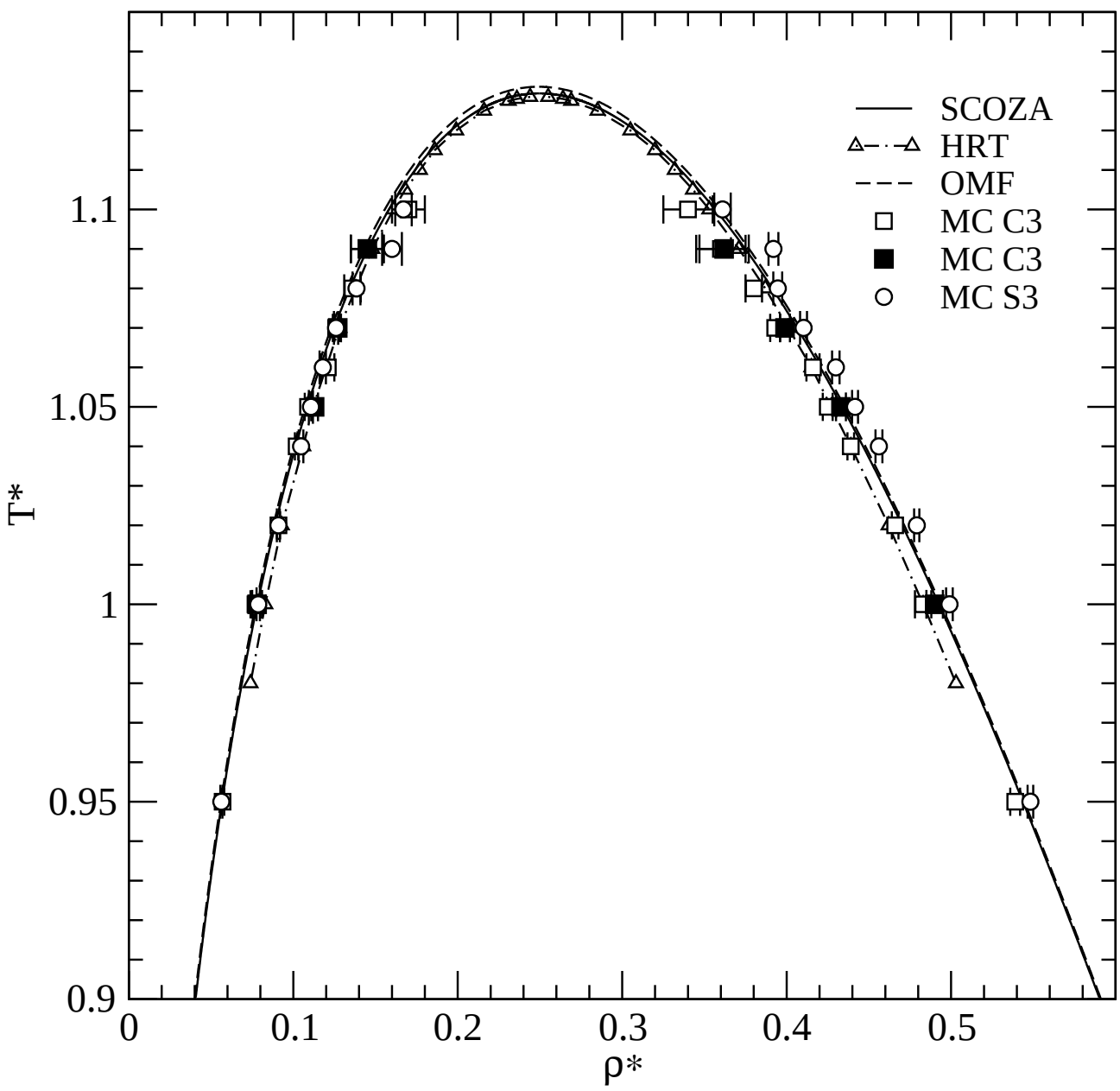

Figure 4. Liquid-vapour coexistence curve of the HCY fluid for $\alpha^* = 0.1$ from SCOZA, HRT and OMF. Simulation results are for the cubic system with EW sums (open squares: $N = 1000$, filled squares: $N = 1872$); and hypersphere calculations (open circles $N = 2000$).

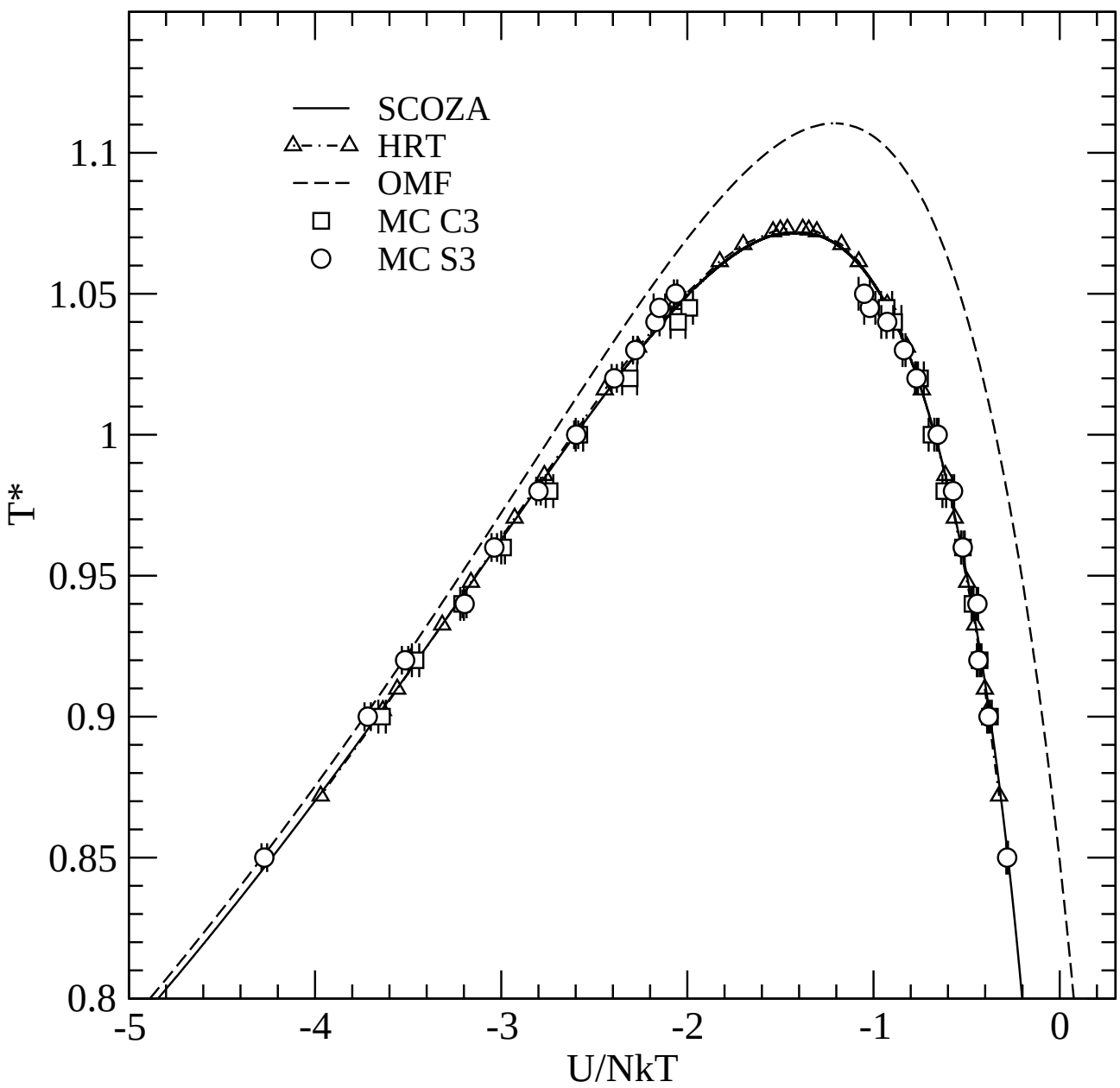

Figure 5. Internal energy $U/Nk_{\mathrm{B}}T$ along the coexistence curve for $\alpha^* = 0.5$. The symbols are as in Fig. 3.

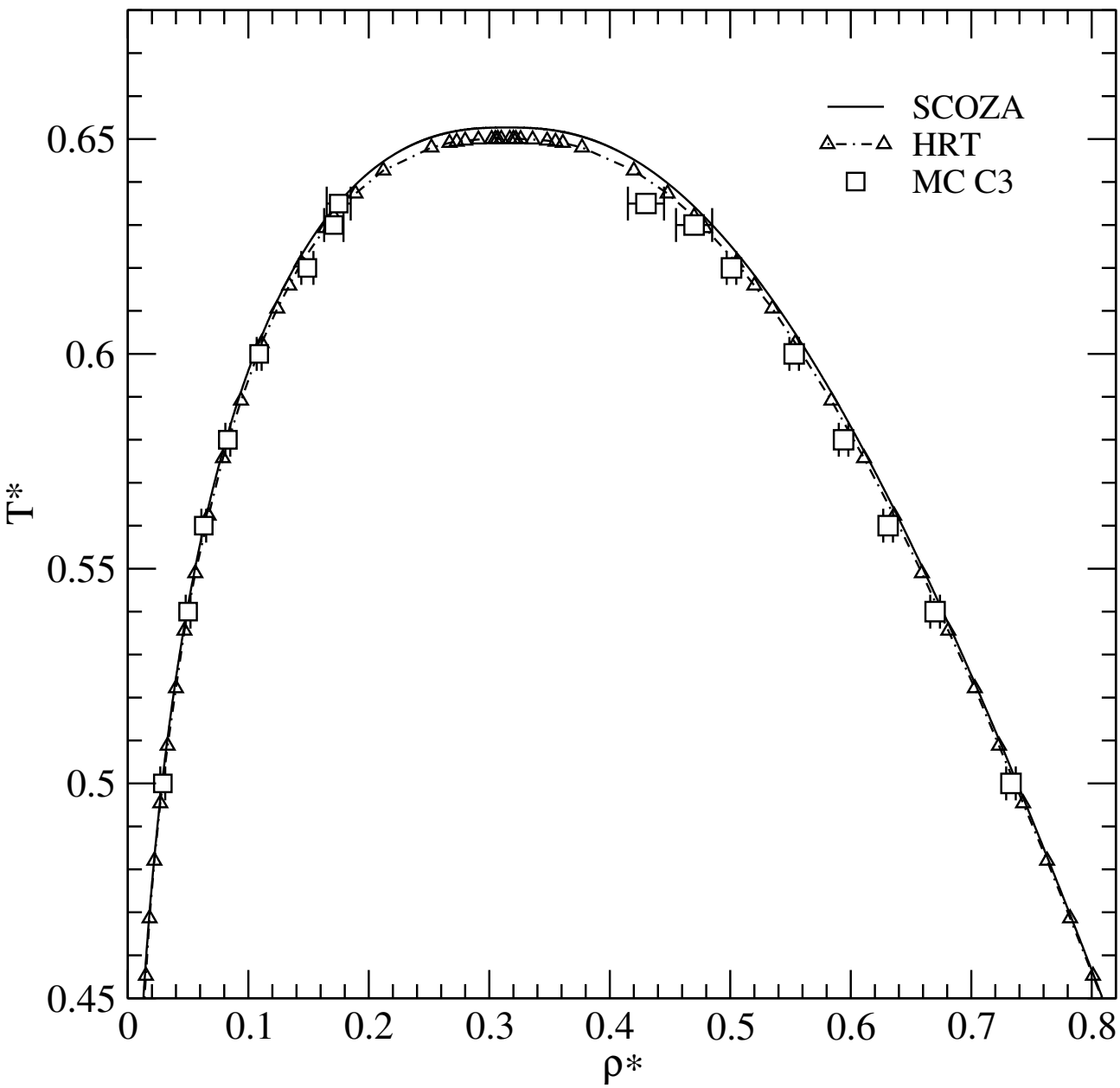
SCOZA
HRT
MC C3
0.65
0.6
0.55
0.5
0.45
T*
0
0.1
0.2
0.3
0.4
0.5
0.6
0.7
0.8
ρ*

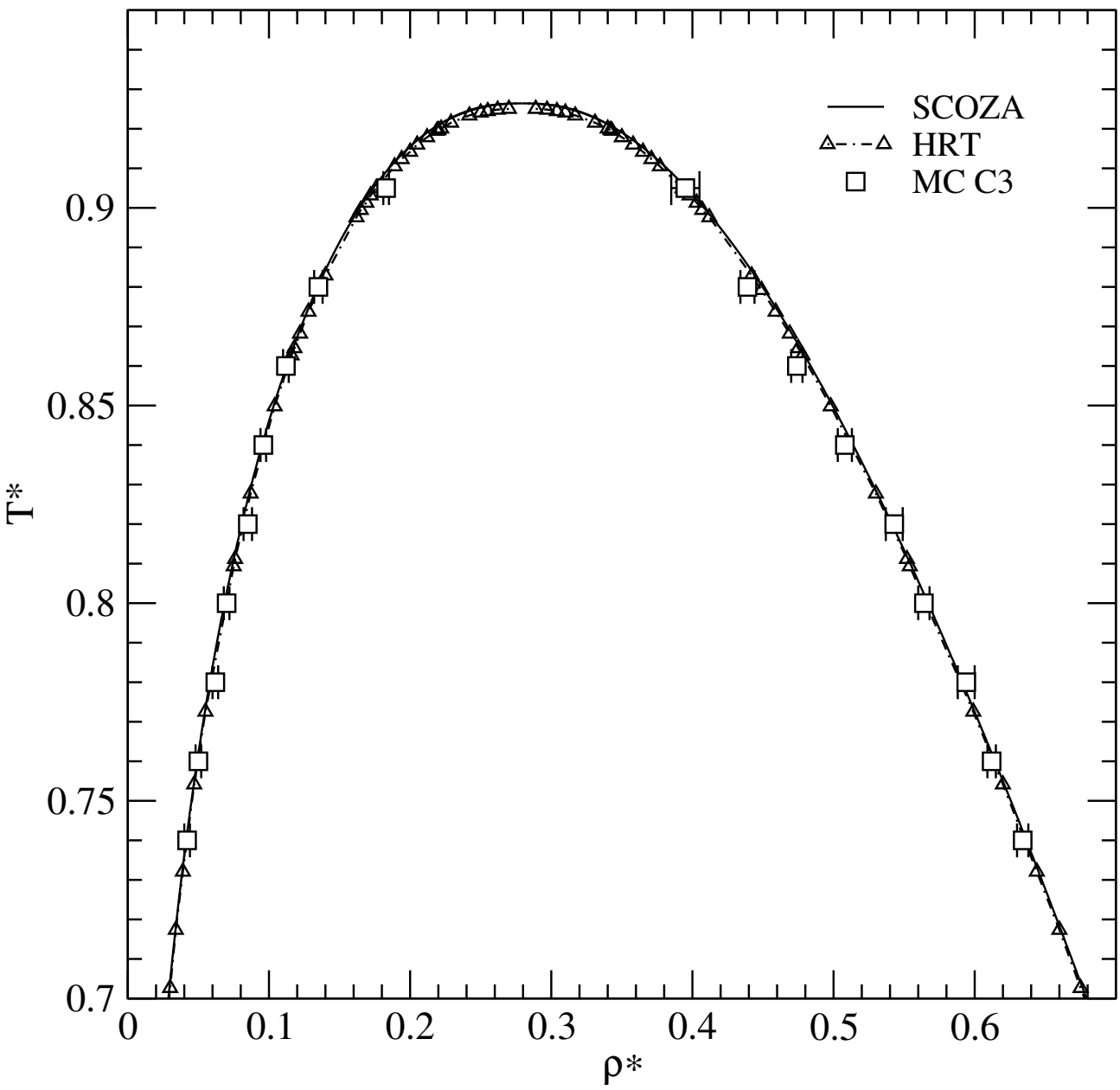
SCOZA
HRT
MC C3
0.9
0.85
0.8
0.75
0.7
T*
0
0.1
0.2
0.3
0.4
0.5
0.6
ρ*

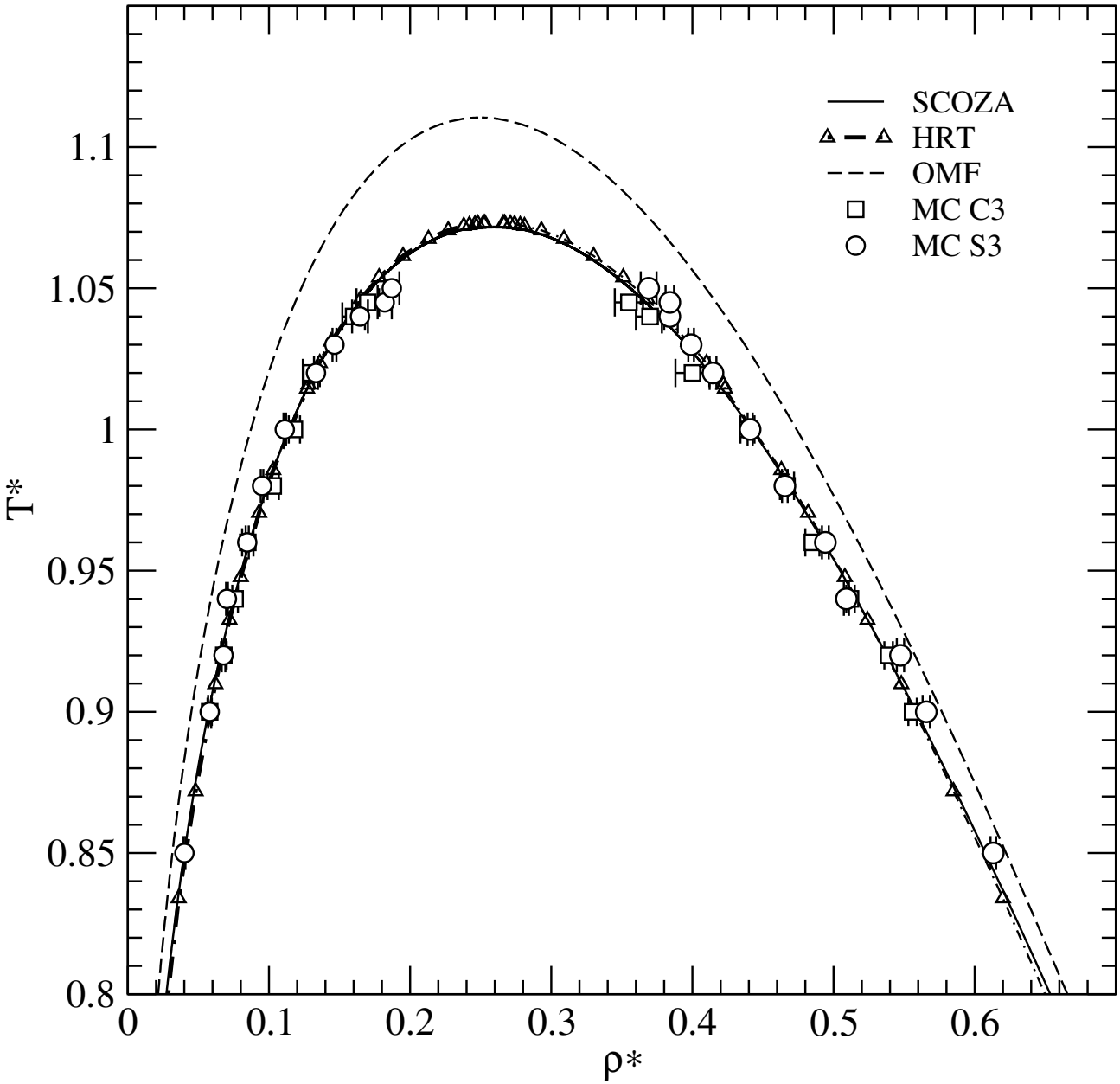
SCOZA
HRT
OMF
MC C3
MC S3
T*
ρ*
1.1
1.05
1
0.95
0.9
0.85
0.8
0
0.1
0.2
0.3
0.4
0.5
0.6

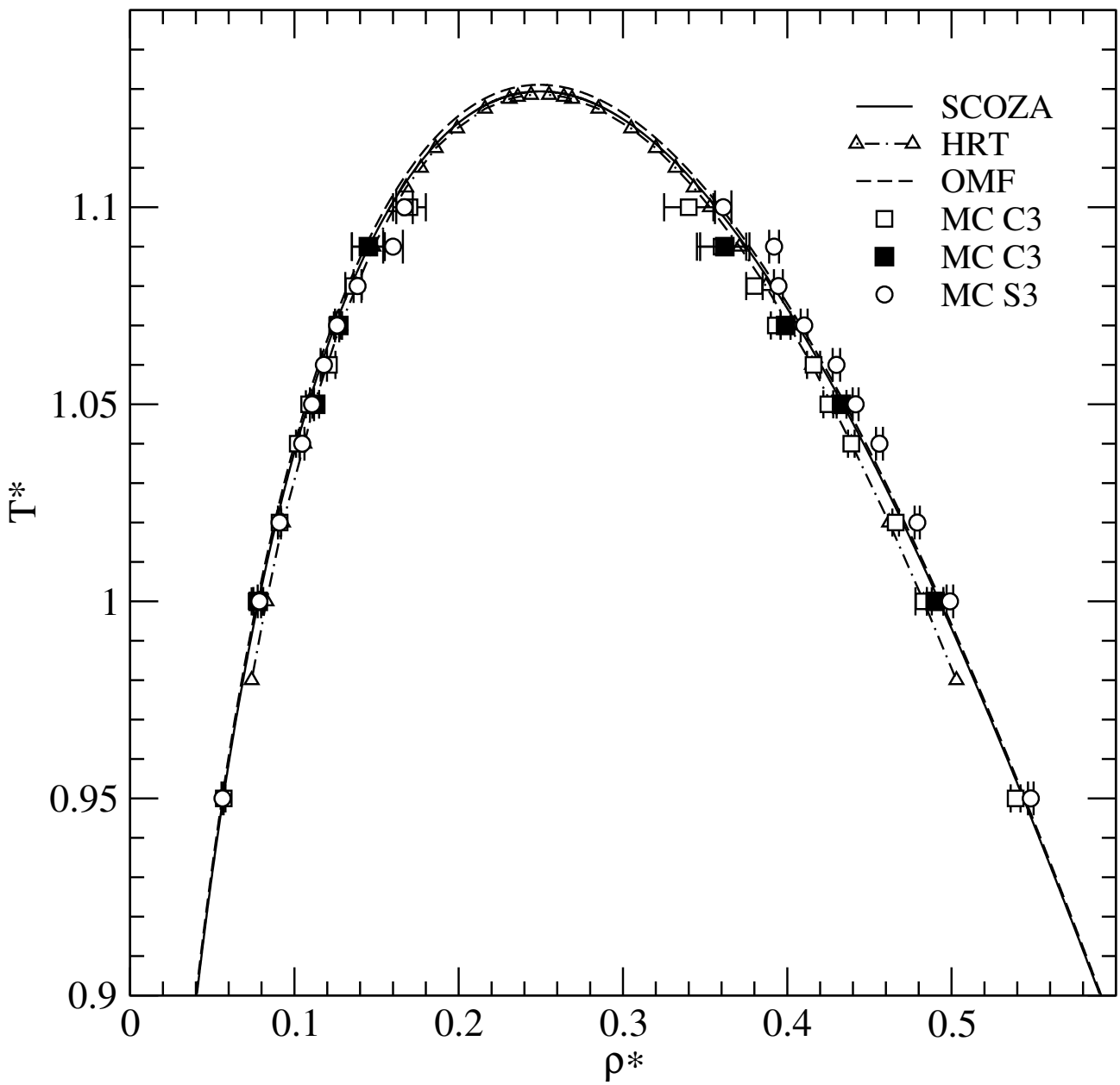
SCOZA
HRT
OMF
MC C3
MC C3
MC S3
T*
ρ*
1.1
1.05
1
0.95
0.9
0
0.1
0.2
0.3
0.4
0.5

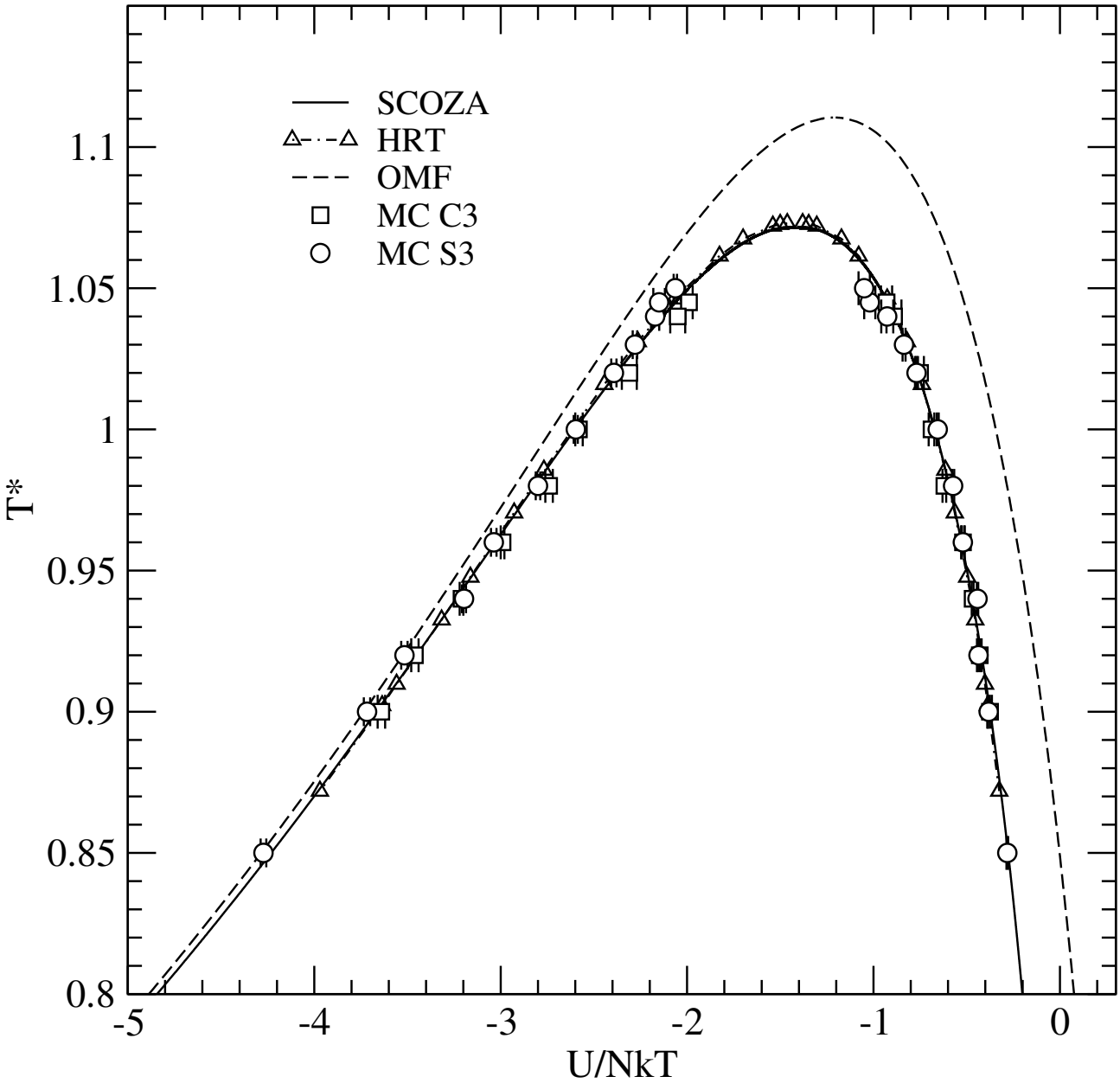
SCOZA
HRT
OMF
MC C3
MC S3
T*
U/NkT
1.1
1.05
1
0.95
0.9
0.85
0.8
-5
-4
-3
-2
-1
0